What Do Ground-Motion Prediction Equations Tell Us About Motions Near Faults?

David M. Boore

Geophysicist

Los Altos, California

Given in the session: Correlations between fault zone structure, earthquakes and generated motion

40th Workshop of the International School of Geophysics on PROPERTIES AND PROCESSES OF CRUSTAL FAULT ZONES

Ettore Majorana Foundation and Centre for Scientific Culture | Erice (TP), Sicily, Italy, May 18-24, 2013

Short Answer: Not Much

- Contents of talk
  - NGA-West 2 Project
    - Develop global database
  - Ground motions near faults
    - Inferring fault slip as a function of space and time (source processes)
    - Spatial variability (source and propagation processes)
  - Scaling of ground motions with magnitude at near and intermediate distances (source processes)
    - Observed scaling
    - Simulated scaling
      - Stochastic simulations
      - Application to simulate M scaling

Pacific Earthquake Engineering Research Center (PEER) Next Generation Attenuation Project (NGA-West 2) Overview

- Goal of Project
  - Derive equations for the prediction of various measures of ground shaking from **crustal earthquakes in active tectonic regions**, as a function of **M**, R, site condition, etc.
- This is the second of two NGA projects. The results of the first project were published in 2008.

Ground-Motion Prediction Equations (GMPEs)

- What are GMPEs?
  - Simple equations giving the mean and standard deviation of measures of ground motion as a function of magnitude, distance, site conditions, and perhaps other variables

- How are GMPEs used?
  - Specify motions for seismic design
    - Individual structures
    - Constructing hazard maps used in building codes
  - Convenient summary of average M and R variation of motion from many recordings
    - Source scaling
    - Path effects
    - Site effects

Ground-Motion Prediction Equations (GMPEs)

$$\ln Y = F_E(\mathbf{M}, mech) + F_{P,B}(R_{JB}, \mathbf{M}) + F_{S,B}(V_{s30}, R_{JB}, \mathbf{M}) + \varepsilon_n \sigma(\mathbf{M}, R_{JB}, V_{S30})$$

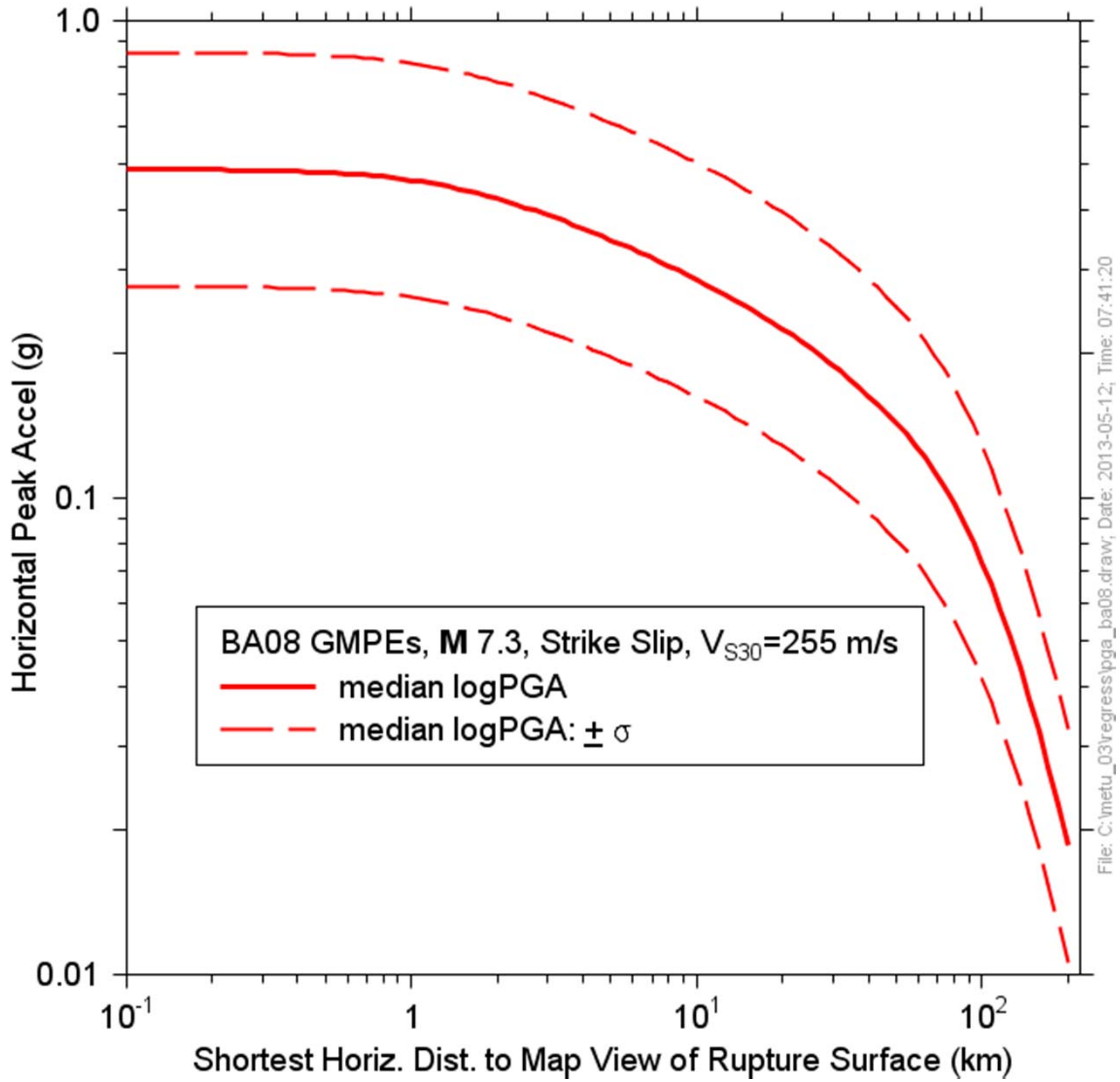

PEER NGA-West 2 Project Overview

- **Developer Teams (each developed their own GMPEs)**
  - Abrahamson, Silva, and Kamae (ASK13)
  - Boore, Stewart, Seyhan, and Atkinson (2 additional members added to the BA08 team) (BSSA13)
  - Campbell & Bozorgnia (CB13)
  - Chiou & Youngs (CY13)
  - Idriss (I13)

- **Supporting Working Groups**
  - Directivity
  - Site Response
  - Database
  - Directionality
  - Uncertainty
  - Vertical Component
  - Adjustment for Damping

PEER NGA-West 2 Project Overview

- All developers used subsets of data chosen from a common database
  - Metadata (e.g., magnitude, distance, etc.)
  - Uniformly processed strong-motion recordings
  - U.S. and foreign earthquakes
  - Active tectonic regions (**subduction, stable continental regions are separate projects**)
- The database development was a major time-consuming effort

NGA-West2 Status

- Most tasks have been completed
  - Databases, damping scaling, directivity, directionality, site response
  - GMPE final reports
- The GMPEs for horizontal components have been submitted to the USGS:
  - Feedback from the USGS National Hazard Maps, internal and external reviewers
- Final reports and the database are now publically available:
  - http://peer.berkeley.edu/ngawest2/final-products/
  - http://peer.berkeley.edu/ngawest2/databases/

Predicted and Predictor Variables

- Ground-motion intensity measures
  - Peak acceleration (PGA)
  - Peak velocity (PGV)
  - Response spectra (PSA, H components combined, similar to geometric mean PSA of the two components)
- Basic predictor variables
  - Moment magnitude (**M**)
  - Distance (R_{JB}, R_{RUP})
  - Site characterization (V_{S30})
- Additional predictor variables
  - Basin depth
  - Hanging wall/foot wall
  - Depth to top of rupture
  - Fault dip
  - Event class (mainshock/aftershock)
  - etc.

Directivity

- NGA-West1 models did not explicitly include directivity of ground motion
- Five directivity models have been developed
  - Wide-band and narrow-band models
- This effort will continue in 2013-14

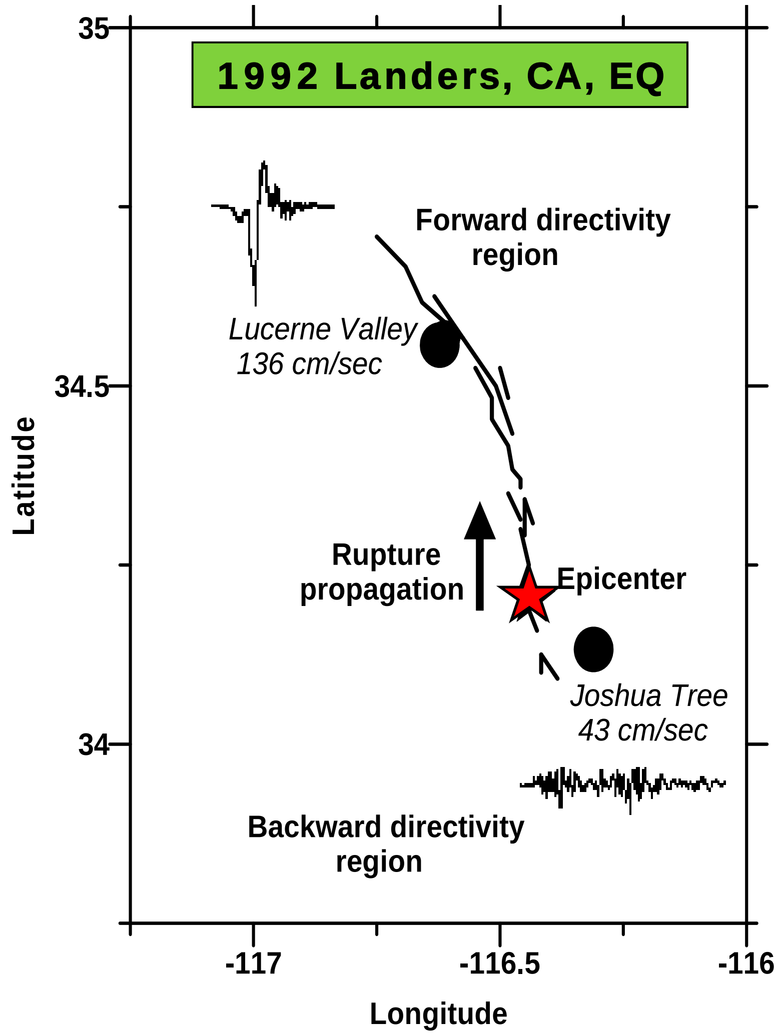

What are response spectra?

- The maximum response of a suite of single degree of freedom (SDOF) damped oscillators for a range of resonant periods, plotted as a function of the resonant period for a given input motion
- Why useful? Buildings can often be represented as SDOF oscillators, so a response spectrum provides the motion of an arbitrary structure to a given input motion, which is useful in engineering design

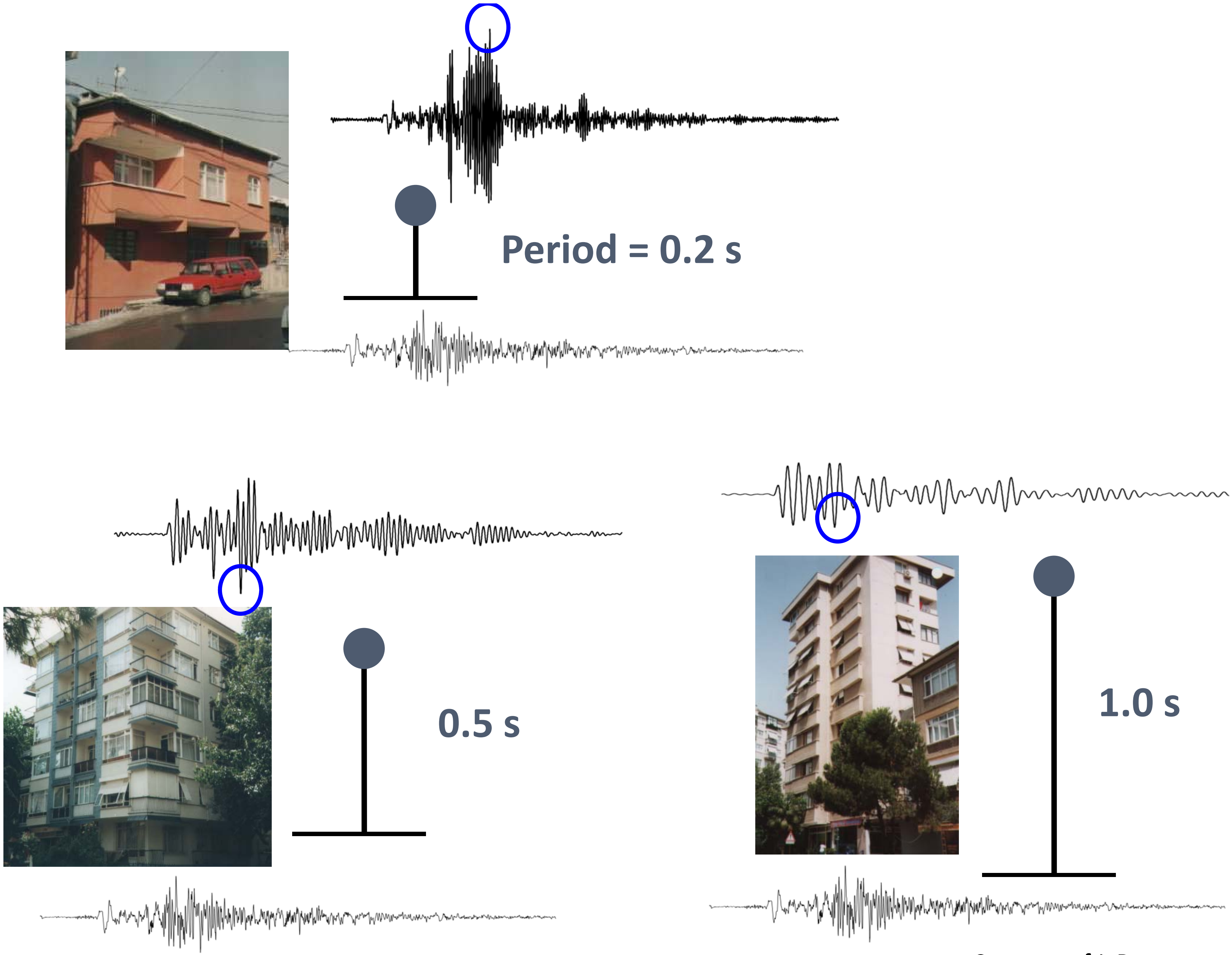

Courtesy of J. Bommer

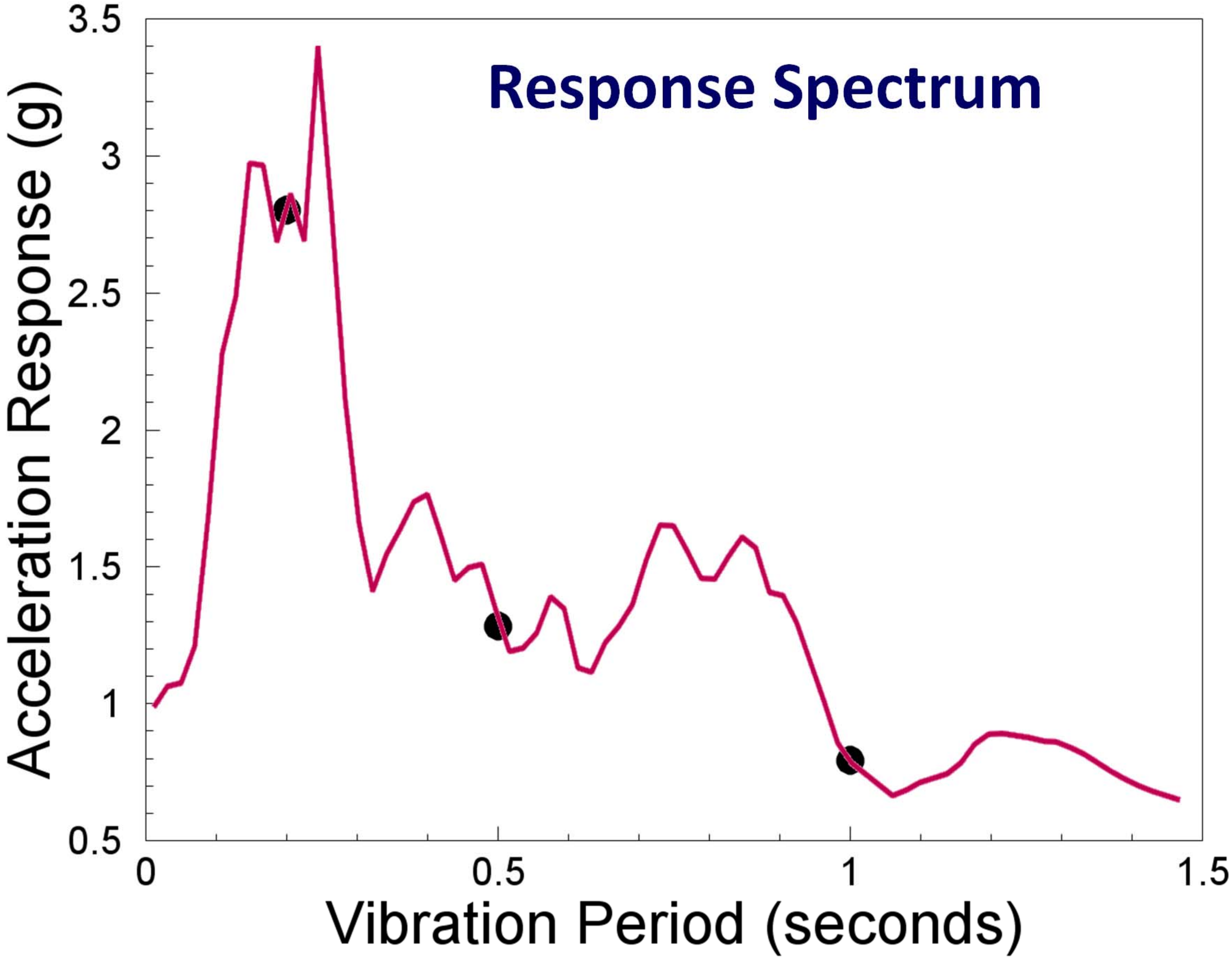

Courtesy of J. Bommer

Distance Measures

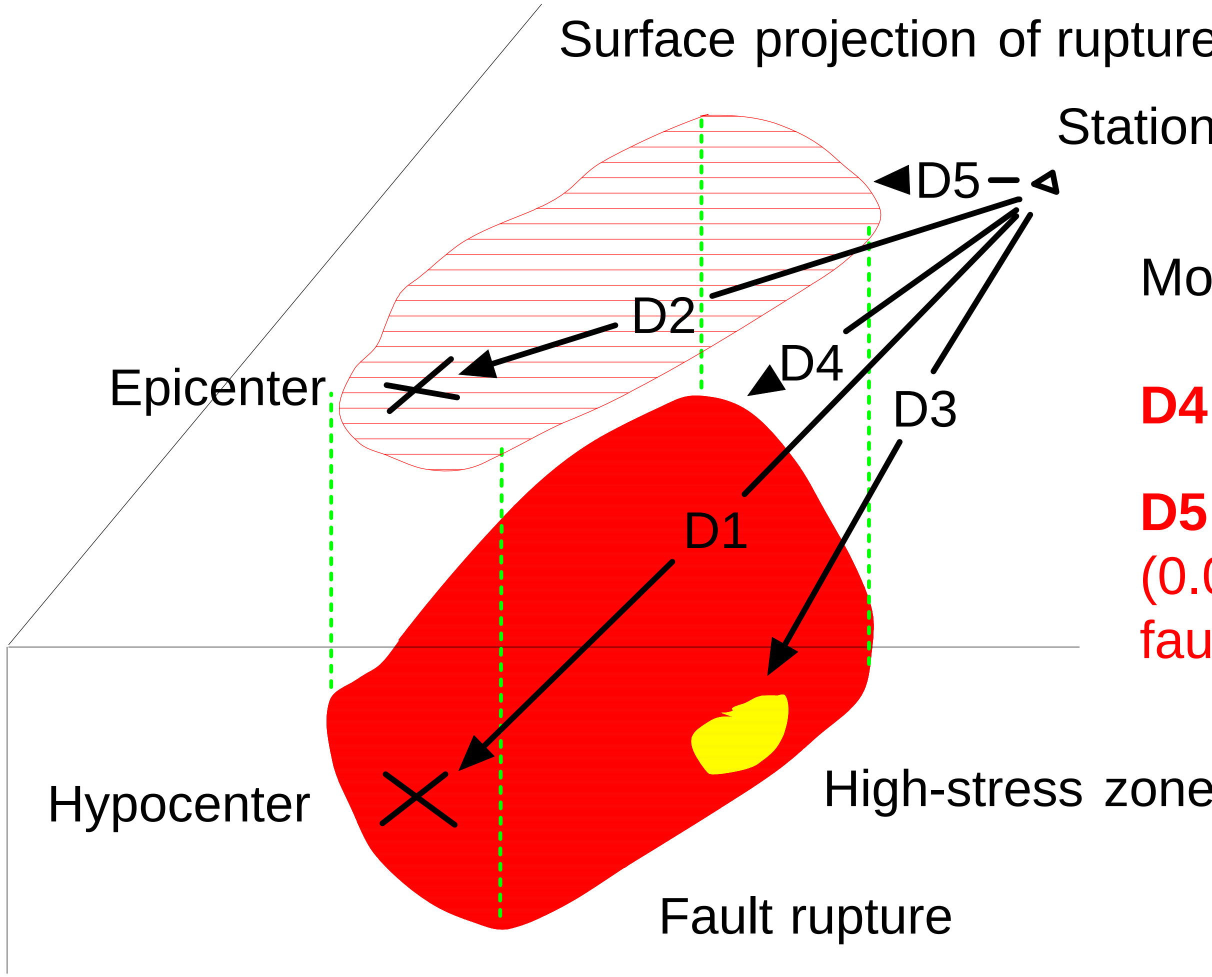

Most Commonly Used:

D4 = R_{RUP}

D5 = R_{JB}
(0.0 for station over the fault)

There are now many networks of strong-motion recorders in the world. Here is an example:

Kyoshin Net (K-NET)
Japanese strong motion network

http://www.k-net.bosai.go.jp

- **1000 digital instruments installed after the Kobe earthquake of 1995**
- **free field stations with an average spacing of 25 km**
- **velocity profile of each station up to 20 m by downhole measurement**
- **data are transmitted to the Control Center and released on Internet in 3-4 hours after the event**
- **more than 2000 accelerograms recorded in 4 years**

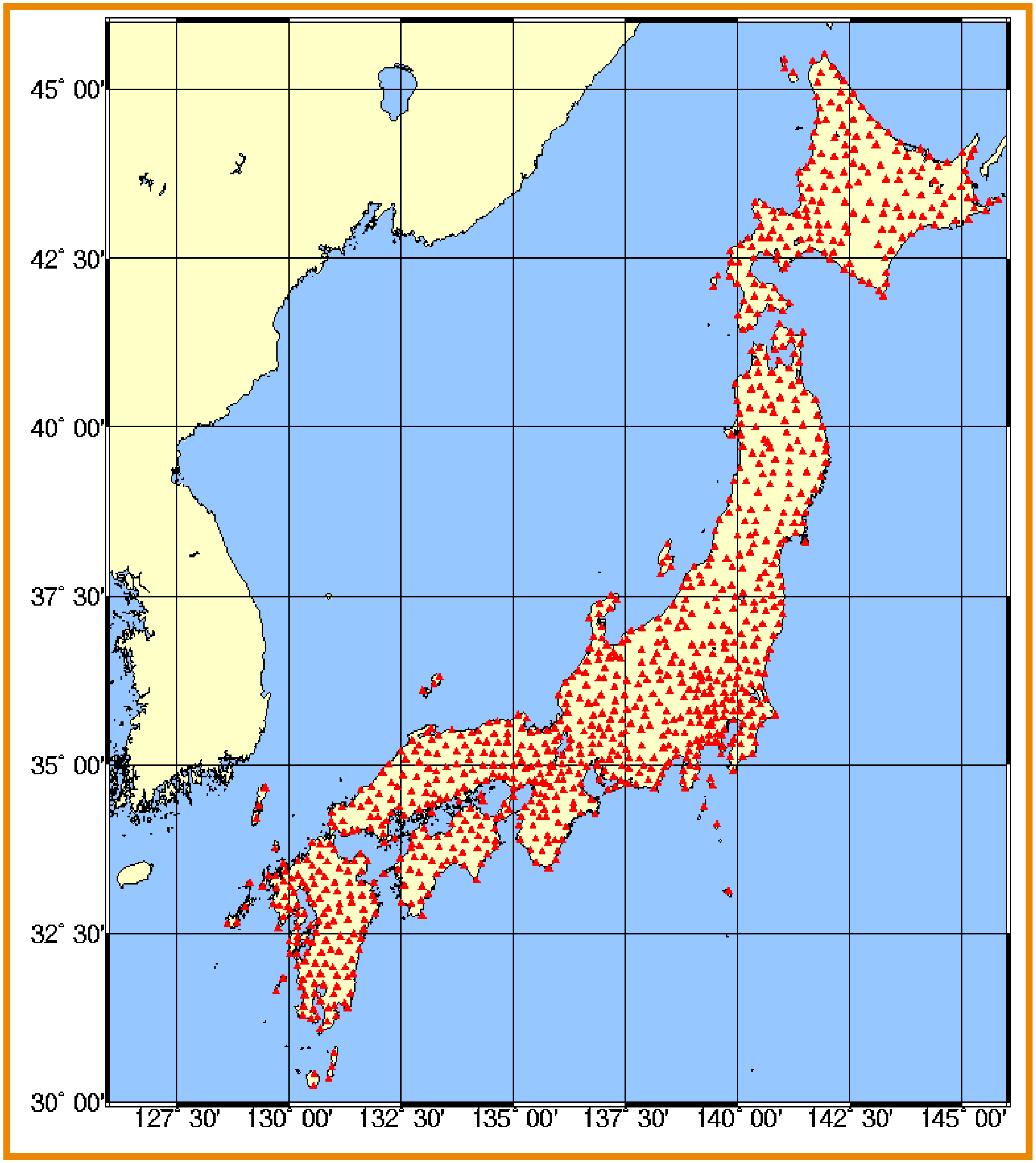

PEER NGA-West 2 Strong-Motion Database

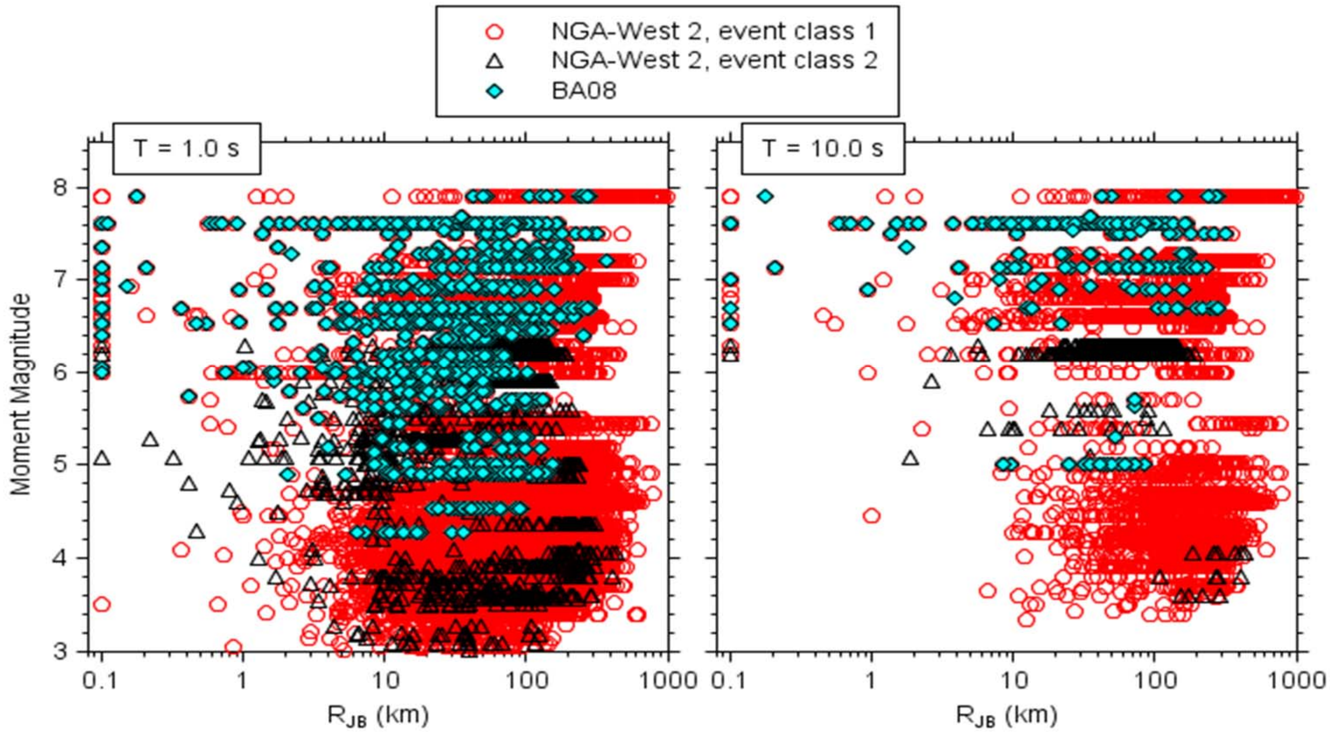

- >600 (173) worldwide shallow crustal events from active tectonic regions
- >21,000 (3551) recordings (mostly 3-components each) uniformly processed strong motion stations
- **M** 3.0 (4.2) to 7.9 (7.9)

Blue = Previous NGA

Examples of data added to NGA-West2 database

Earthquake Name*	Year	M	N Rec	Rrup Range (km)
Tottori, Japan	2000	6.6	414	1-333
Niigata, Japan	2004	6.6	530	8-300
Chuetsu-oki, Japan	2007	6.8	616	10-300
Iwate, Japan	2008	6.9	367	5-280
El Mayor-Cucapah, CA	2010	7.2	238	11-240
Darfield, New Zealand	2010	7.0	114	1-540
Christchurch, New Zealand	2011	6.1	104	2-440
Wenchuan, China	2008	7.9	263	1-1500
L'Aquila, Italy	2009	6.3	48	5-230

*subset of added events

How the NGA-West 2 Project Fits into this Talk

- The database created in the project contains uniformly processed data and carefully screened metadata (e.g., V_{S30}) that can be used in studies of near-fault ground motions
  - Amplitude variations
  - Polarization complexities
- The GMPEs provide a summary of many data (used for studies of source, path, and site effects)
  - Scaling with magnitude

Ground Motions Near Faults

Large Earthquakes with Near-Fault Recordings of Ground Motion

- 1999 Kocaeli, Turkey (**M** 7.5)
- 1999 Chi-Chi, Taiwan (**M** 7.6)
- 1999 Duzce, Turkey (**M** 7.1)
- 2002 Denali Fault, Alaska (**M** 7.9)
- 2004 Parkfield, California (**M** 6.0)
- 2008 Wenchuan, China (**M** 7.9)

Numbers of Records in PEER NGA-West 2 Database for 3 Near-fault Distance Ranges

Event	Type	M	R_{JB}<2 km	R_{JB}<5 km	R_{JB}<10 km
Kocaeli	SS	7.6	2	3	4
Chi-Chi	RS	7.5	18	23	42
Duzce	SS	7.1	2	7	9
Denali	SS	7.9	1	1	1
Parkfield	SS	6.0	19	41	63
Wenchuan	RS	7.9	5	6	6

Note that being close is not the same as being in the fault zone. This is particularly true for non-vertical faults (usually RS, NS faults). It is also true that a station can be in the Fault Damage Zone, and yet R_{JB} could be large. The dataset available to me did not have a variable indicating whether or not a station was in the FDZ.

Near-fault records are usually used in determinations of fault slip as a function of space and time: the 1999 Kocaeli, Turkey (**M** 7.5)

From Bouchon et al. (2002)

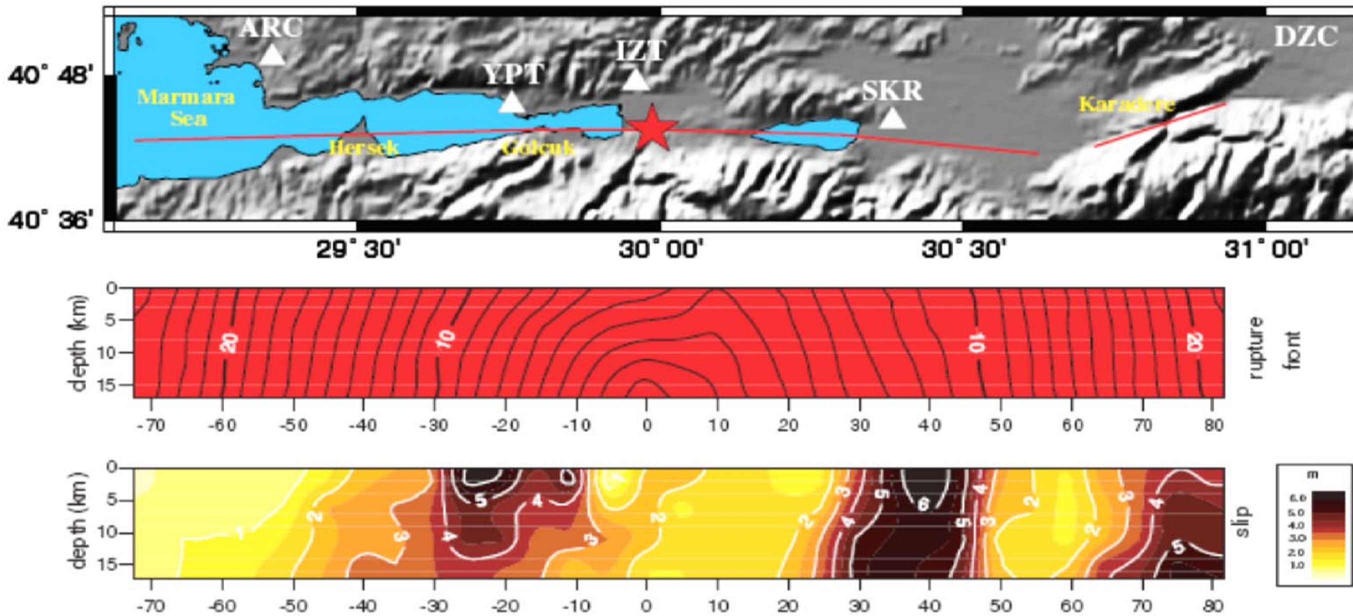

From Liu et al. (2006)

2004 Parkfield, California (**M** 6.0)

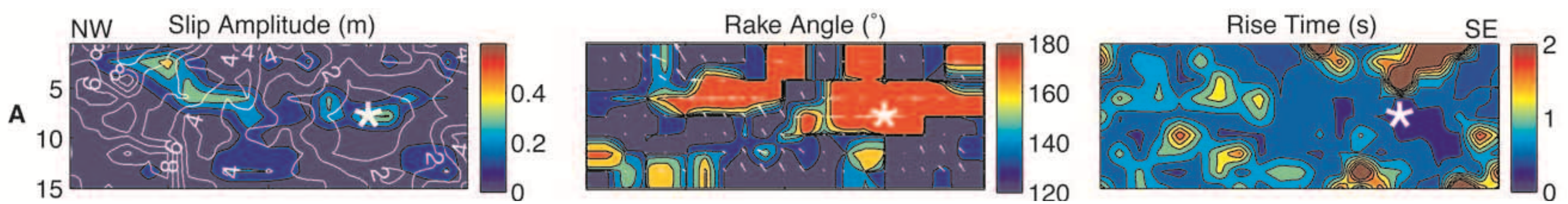

The records also tell us about spatial variability of motions near faults

Parkfield
2004

Most Extensively Observed Earthquake to Date in the Near-Fault Region

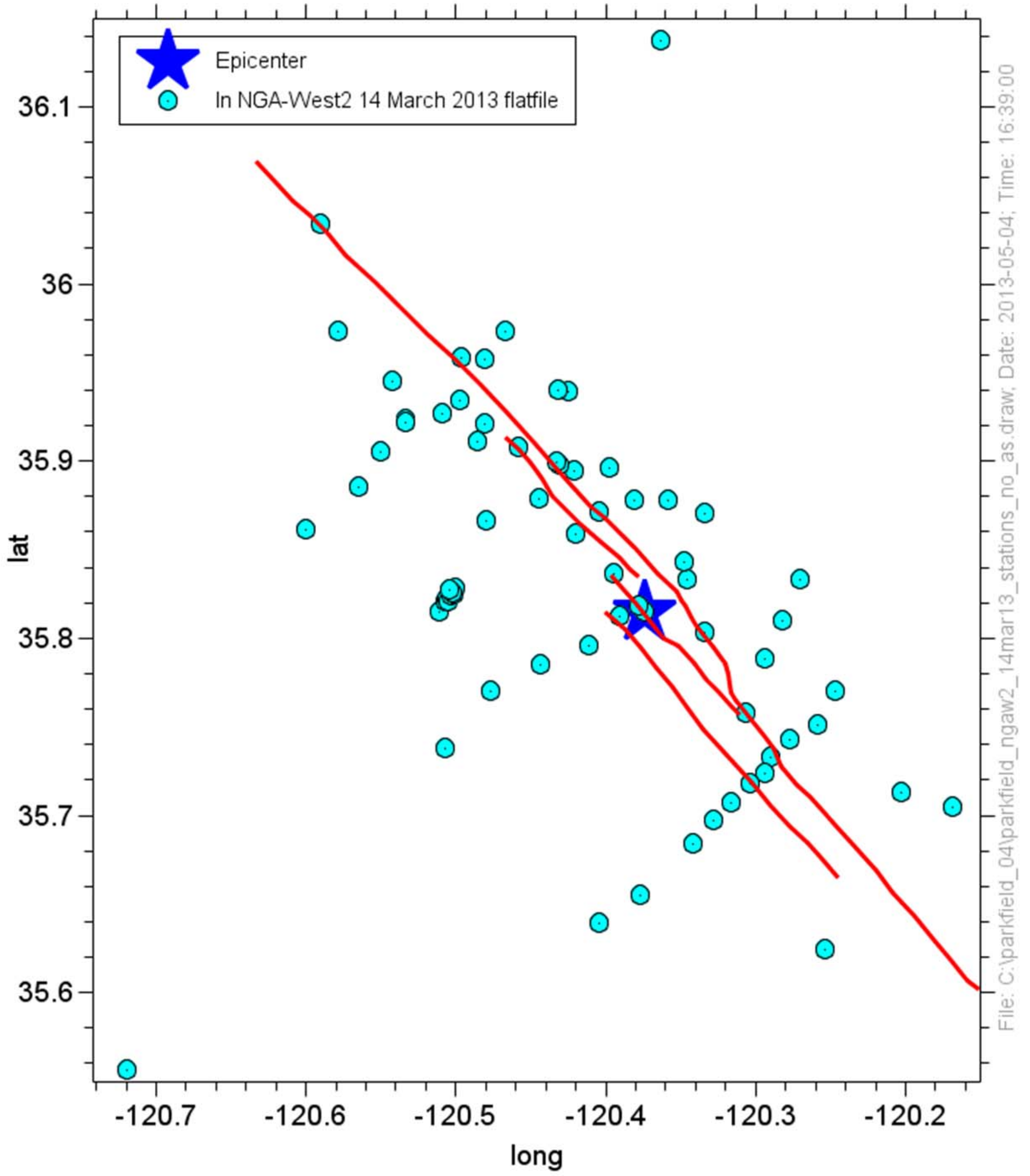

Coherent polarization and spatial variations in amplitude for displacements

Figure 14. Displacement particle motions calculated from the recorded accelerations at each station. The motions in the central part of the faulting are mostly low, and largest at the ends. The simplified line source fault model used in determining fault distances is shown for reference (end points 35.784° N, 120.334° W and 36.005° N, 120.562° W).

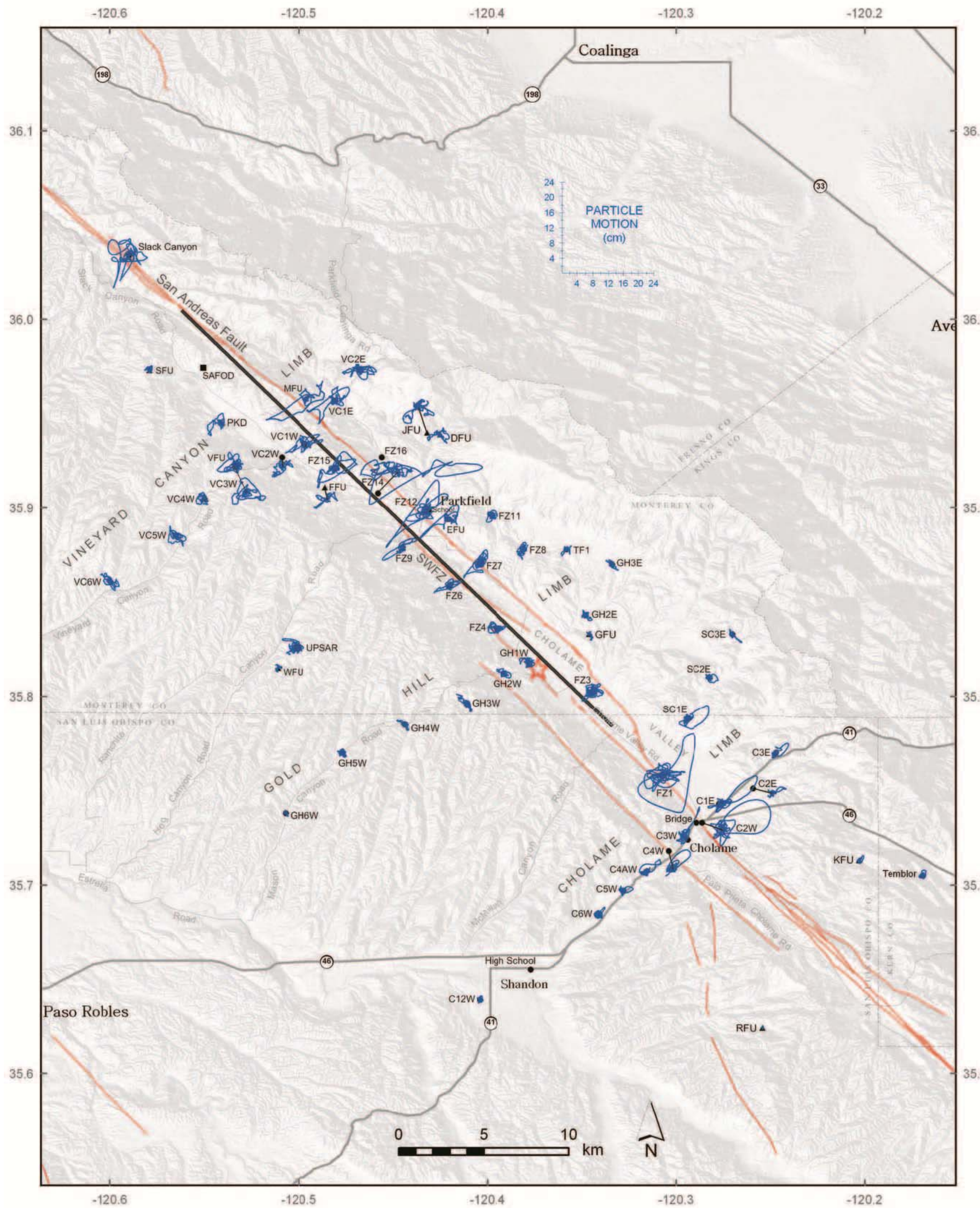

Shakal et al. (2006a)

Sources of Variability

- Nonuniform fault slip
- Site geology
- Fault zone effects
- See Antonio Rovelli's talk for more discussion of the sources of variability

The records also tell us about spatial variability of motions near faults

Parkfield
2004

Most Extensively Observed Earthquake to Date in the Near-Fault Region

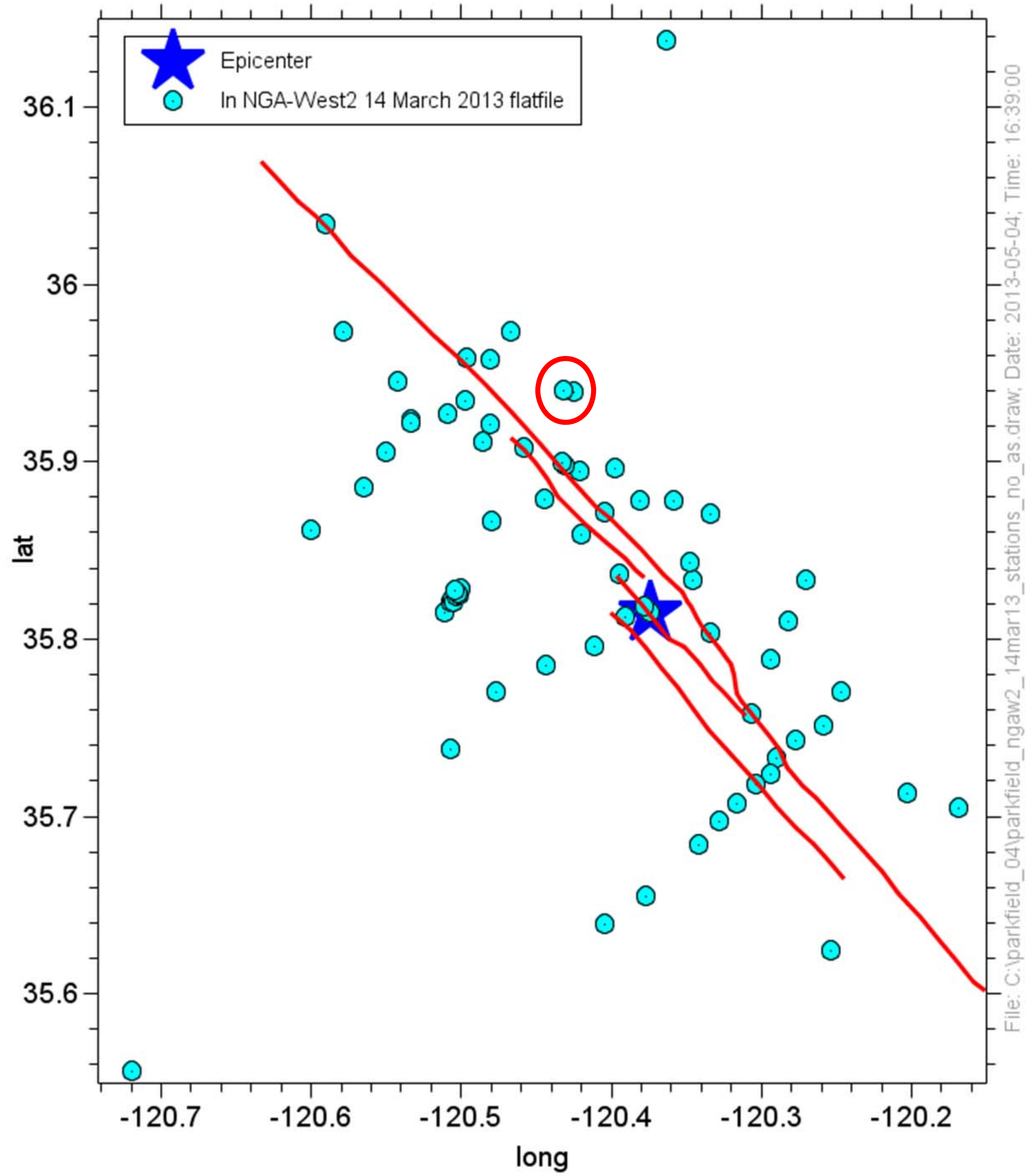

Spatial variations depend on frequency content of the motion—for a given station separation, expect more variability for higher frequency motions

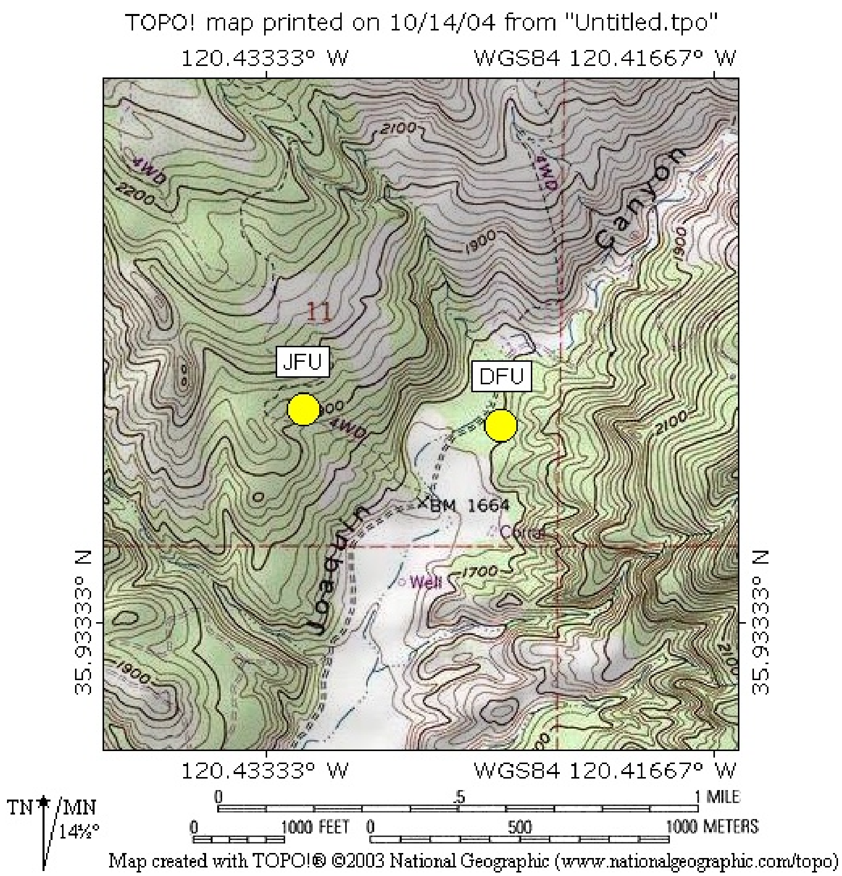

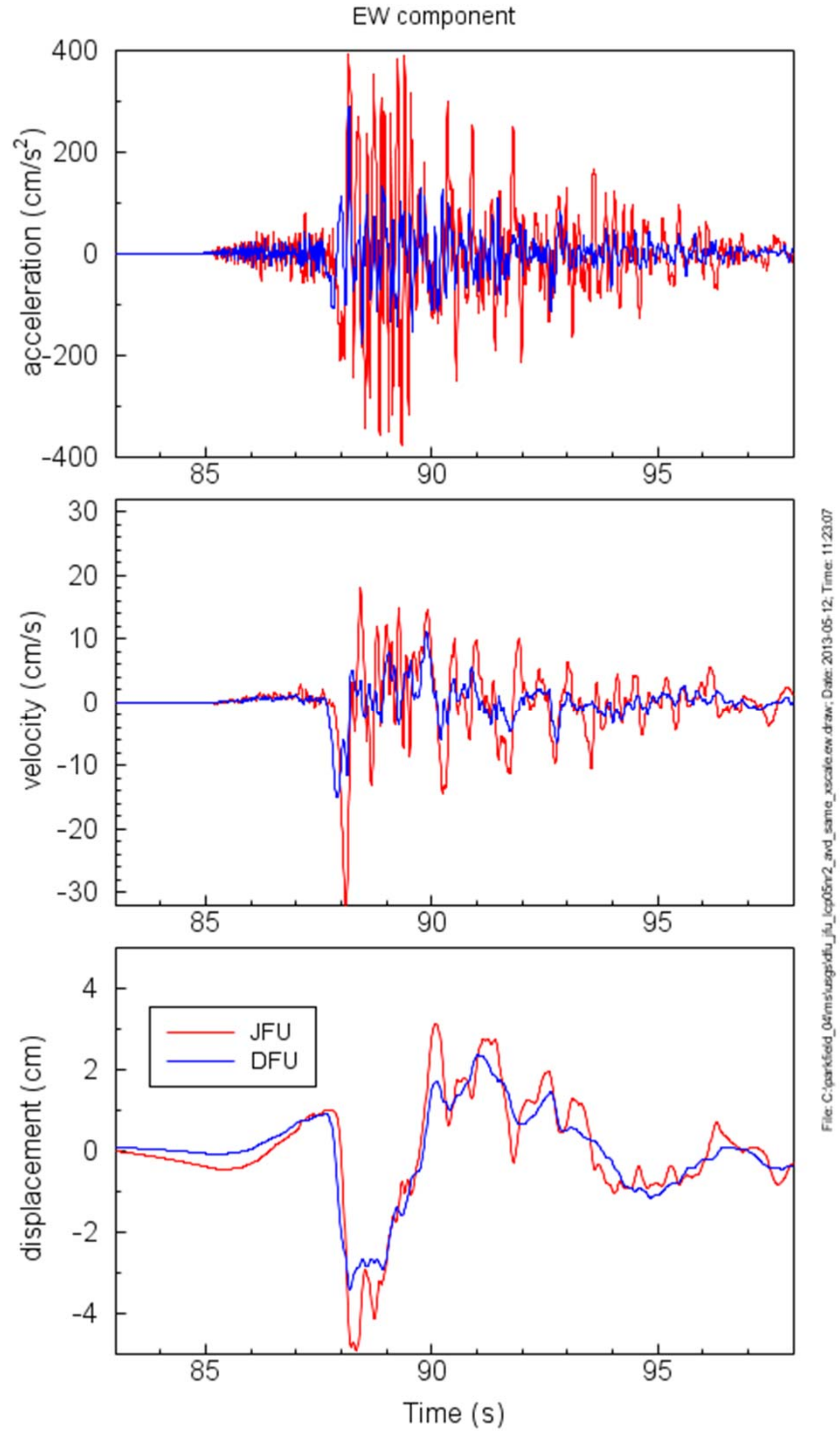

The records also tell us about spatial variability of motions near faults

Parkfield
2004

Most Extensively Observed Earthquake to Date in the Near-Fault Region

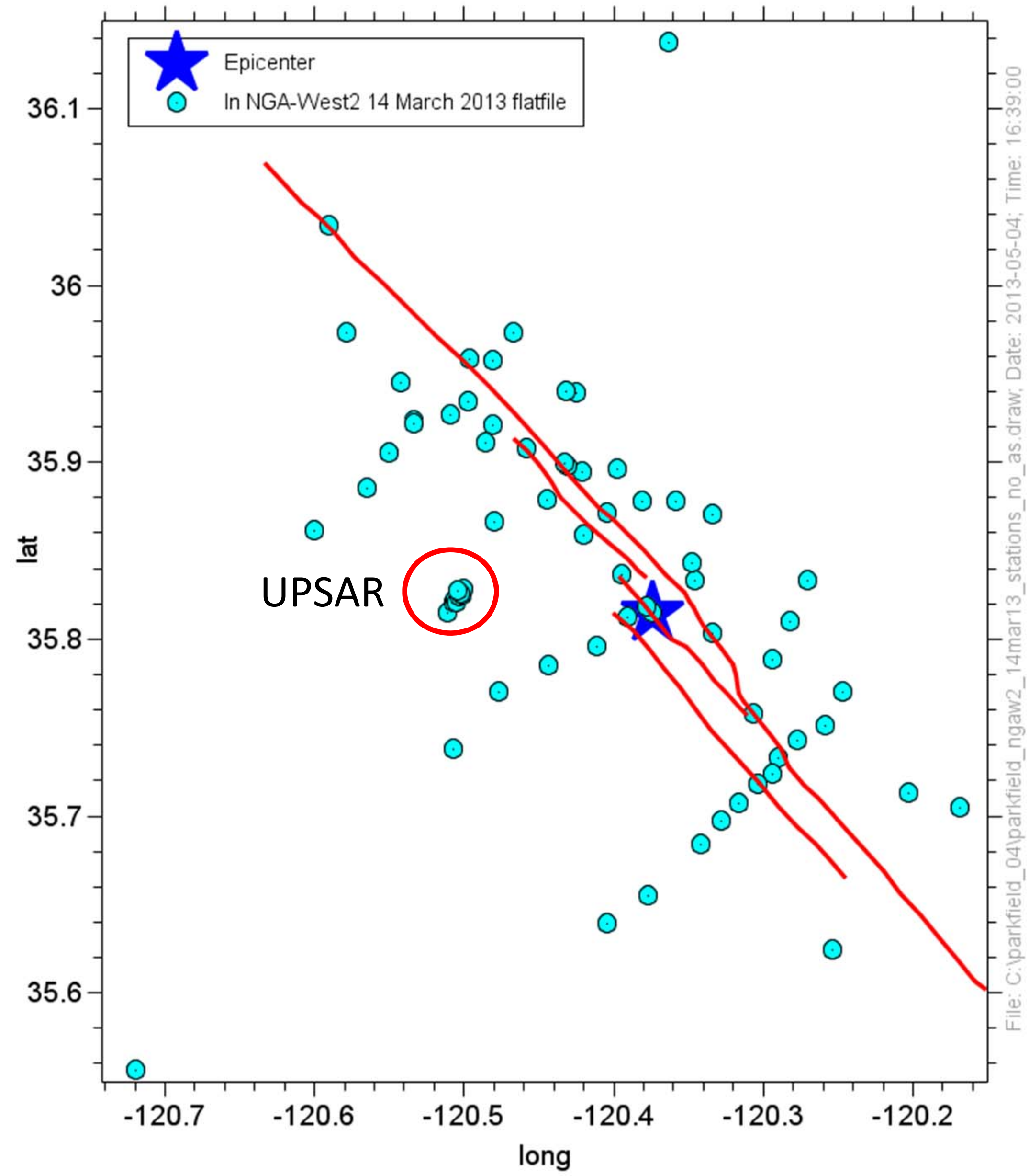

USGS Parkfield Dense Seismograph Array (UPSAR) Recordings of the 2004 Parkfield Earthquake

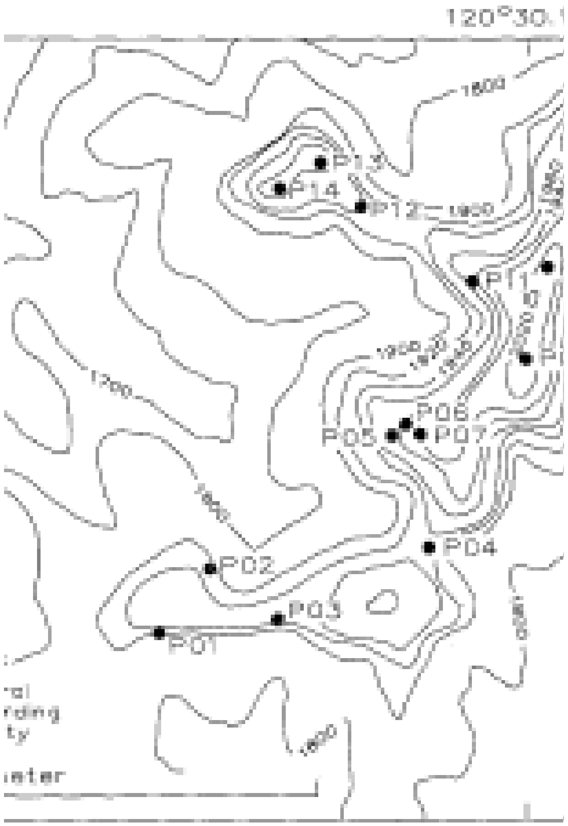

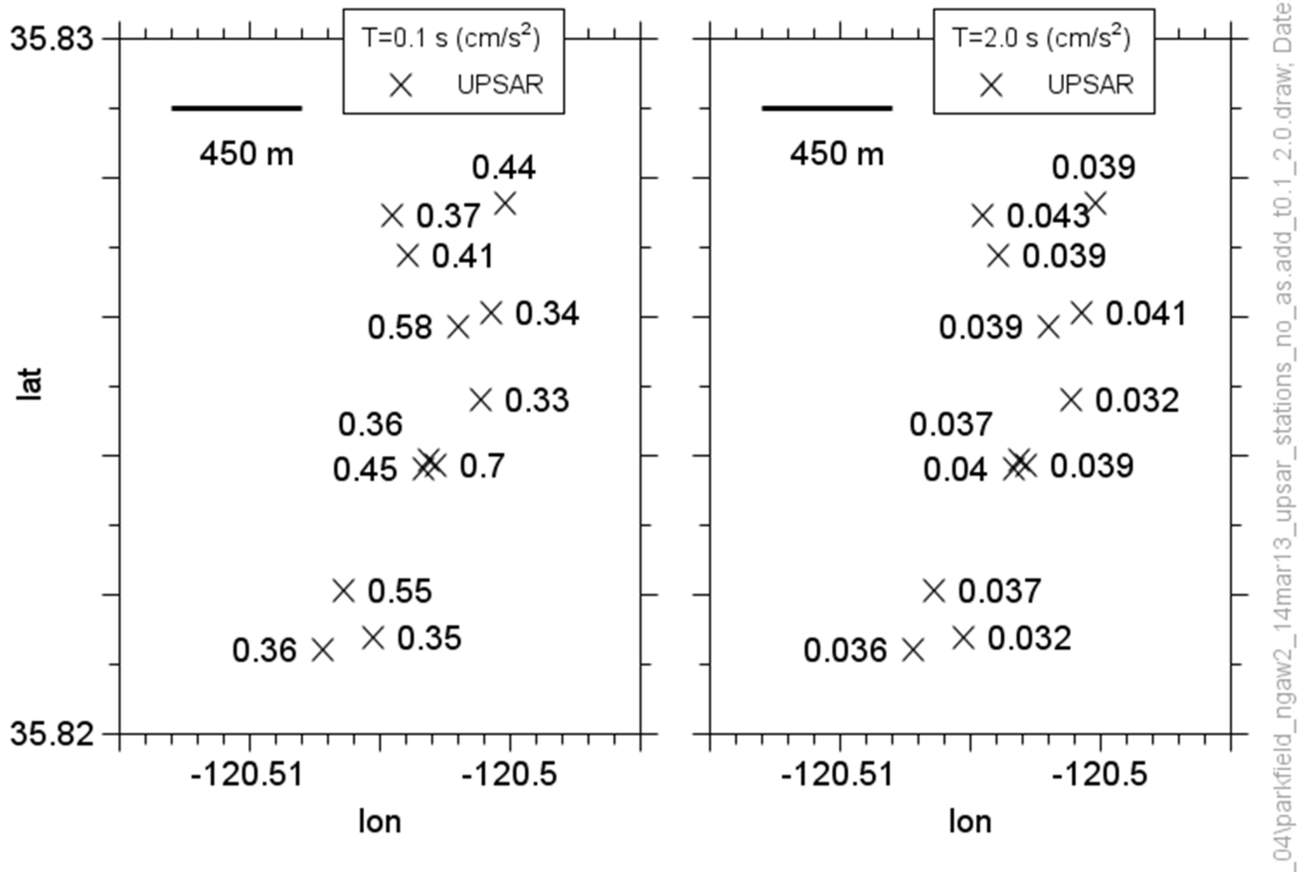

Less variability for longer period motion

From Fletcher et al. (1992)

T=0.1 s

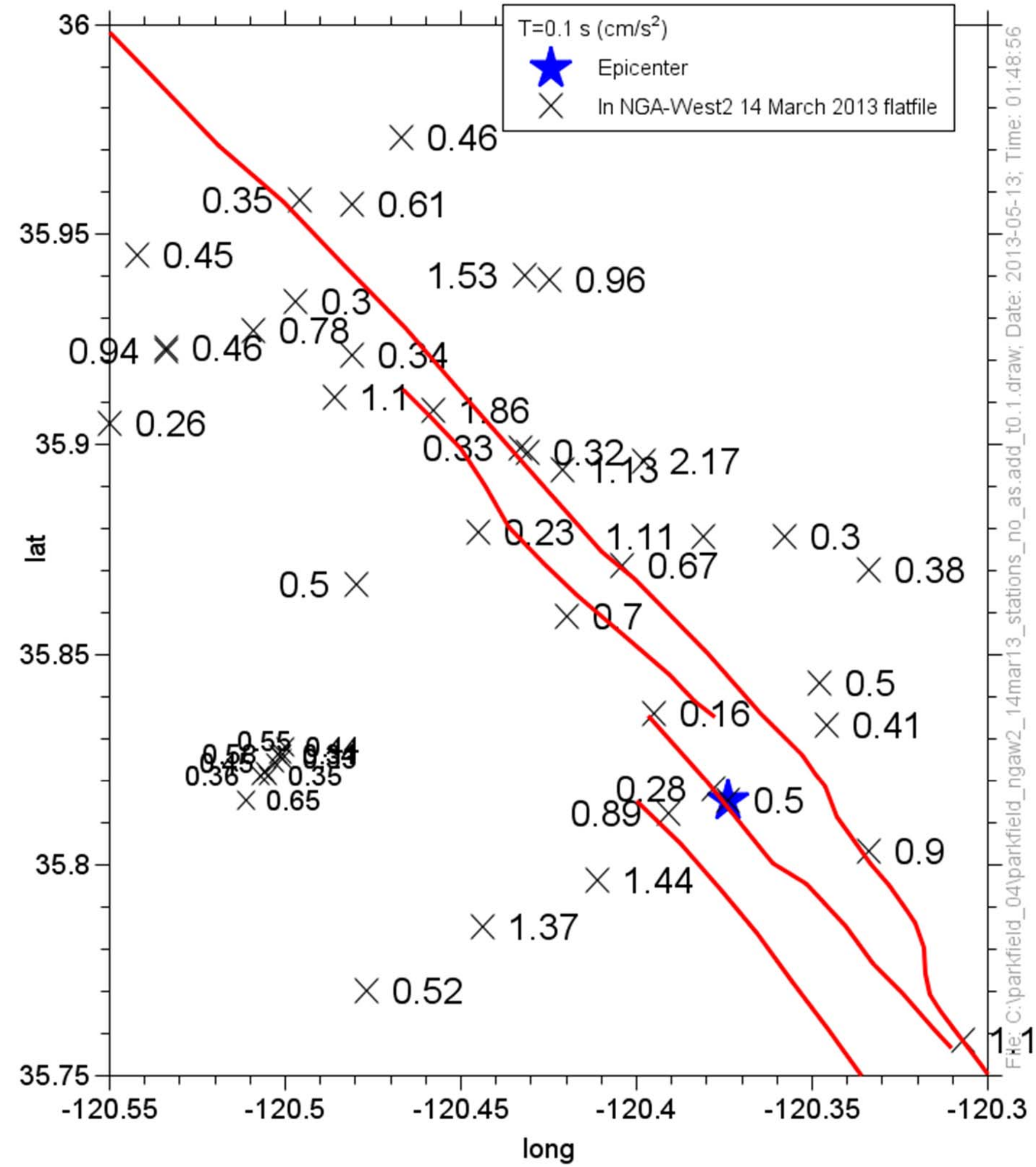

T=0.1 s (cm/s²)
Epicenter
In NGA-West2 14 March 2013 flatfile
lat
long
36
35.95
35.9
35.85
35.8
35.75
-120.55
-120.5
-120.45
-120.4
-120.35
-120.3
File: C:\parkfield_04\parkfield_ngaw2_14mar13_stations_no_as.add_t0.1.draw; Date: 2013-05-13; Time: 01:48:56
0.46
0.35
0.61
0.45
1.53
0.96
0.3
0.78
0.94
0.46
0.34
1.1
1.86
0.26
0.33
0.32
1.13
2.17
0.23
1.11
0.3
0.67
0.38
0.5
0.7
0.5
0.16
0.41
0.35
0.65
0.28
0.5
0.89
0.9
1.44
1.37
0.52
1.1

T=2.0 s

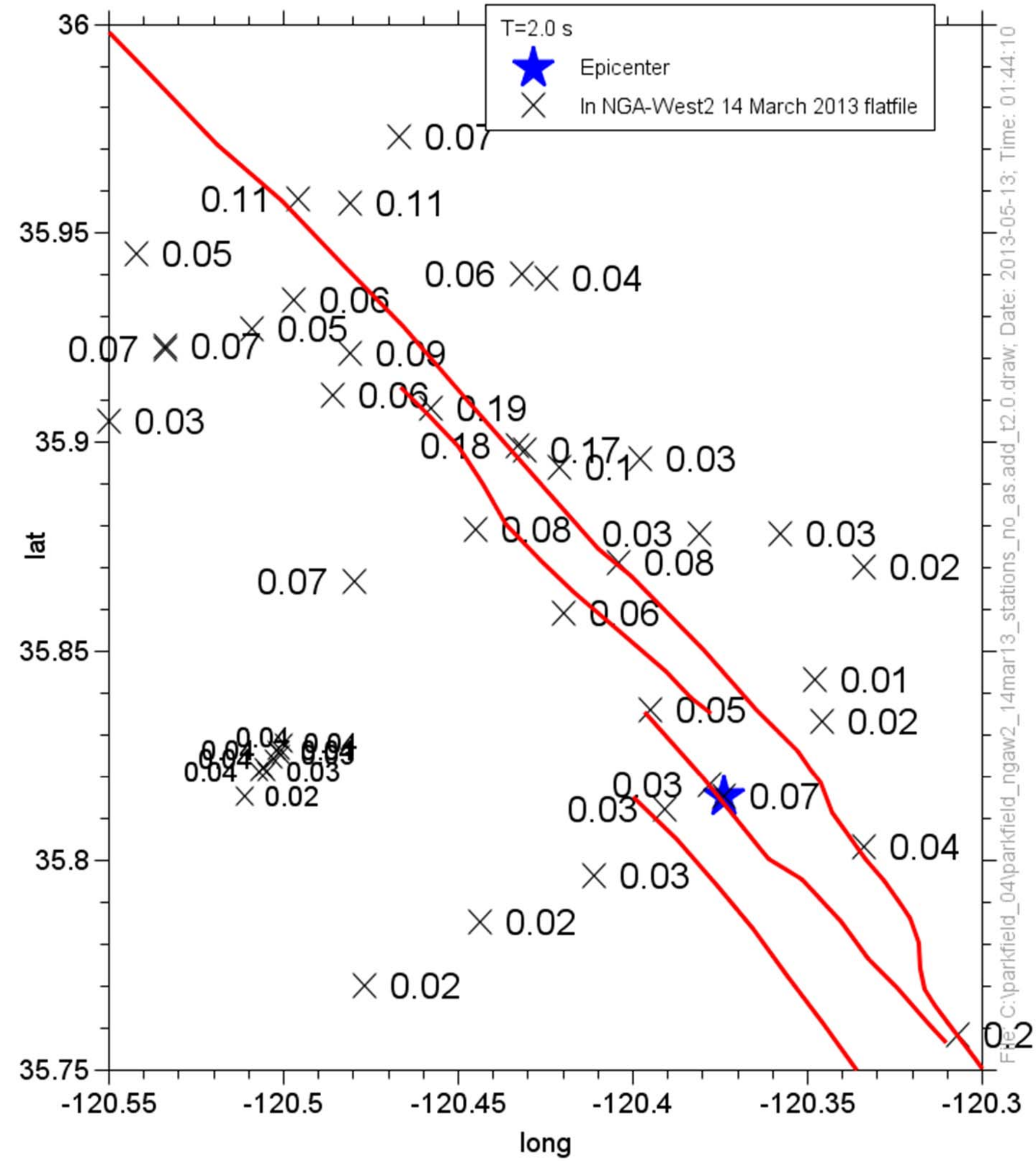

T=2.0 s
Epicenter
In NGA-West2 14 March 2013 flatfile
lat
long
36
35.95
35.9
35.85
35.8
35.75
-120.55
-120.5
-120.45
-120.4
-120.35
-120.3
0.07
0.11
0.11
0.05
0.06
0.04
0.06
0.05
0.07
0.07
0.09
0.06
0.19
0.03
0.18
0.17
0.1
0.03
0.08
0.03
0.03
0.08
0.02
0.07
0.06
0.01
0.05
0.02
0.02
0.03
0.07
0.03
0.04
0.03
0.02
0.02
0.2
File: C:\parkfield_04\parkfield_ngaw2_14mar13_stations_no_as.add_t2.0.draw; Date: 2013-05-13; Time: 01:44:10

Recordings near the Calaveras Fault Zone

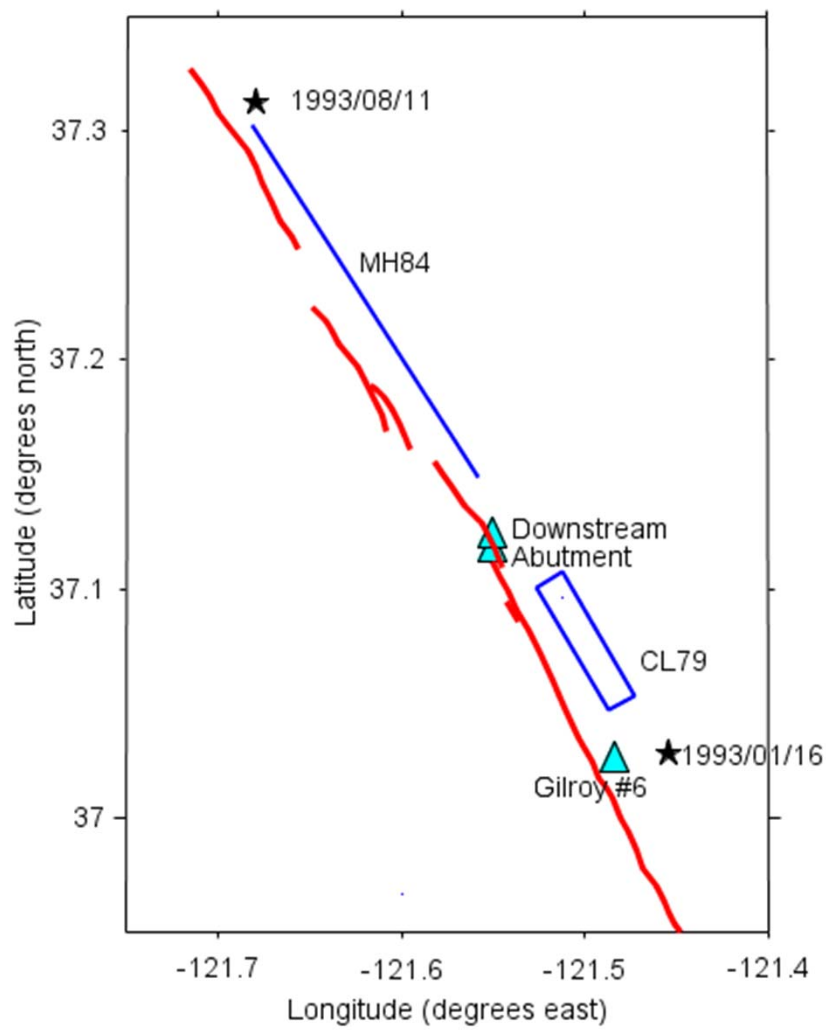

Coyote Lake downstream in the fault zone with Vs30=295 m/s

Gilroy #6 on a ridge to the east of the fault, with Vs30=663 m/s

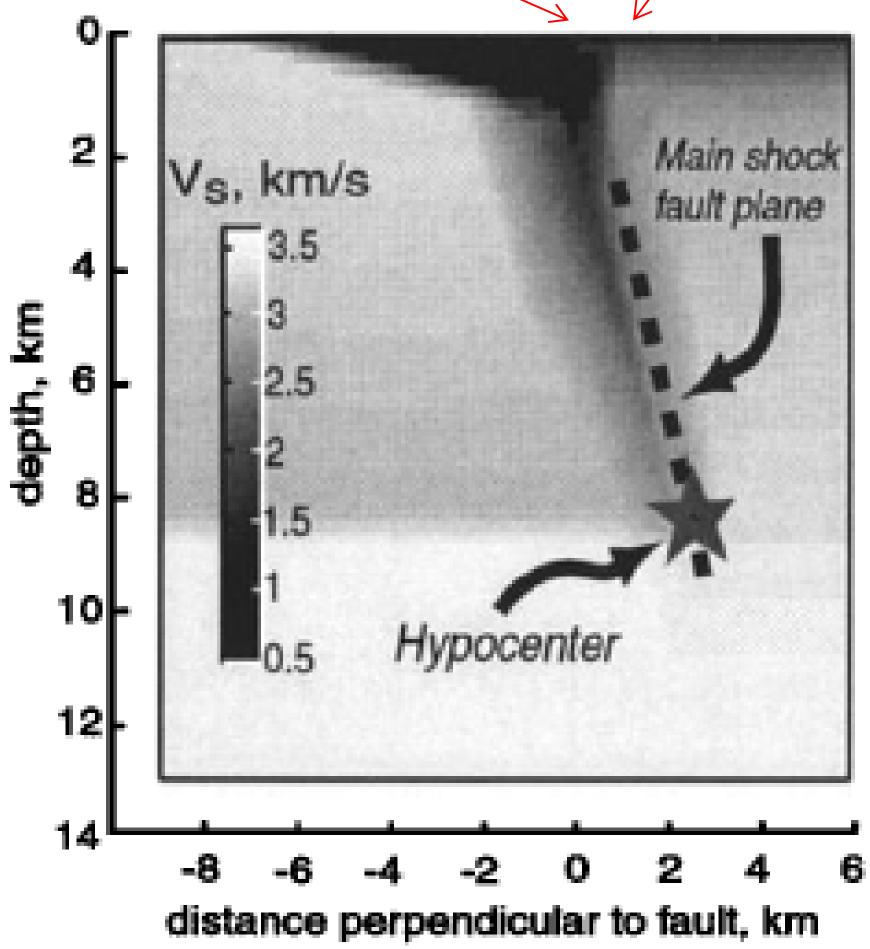

From Spudich and Olsen (2001)

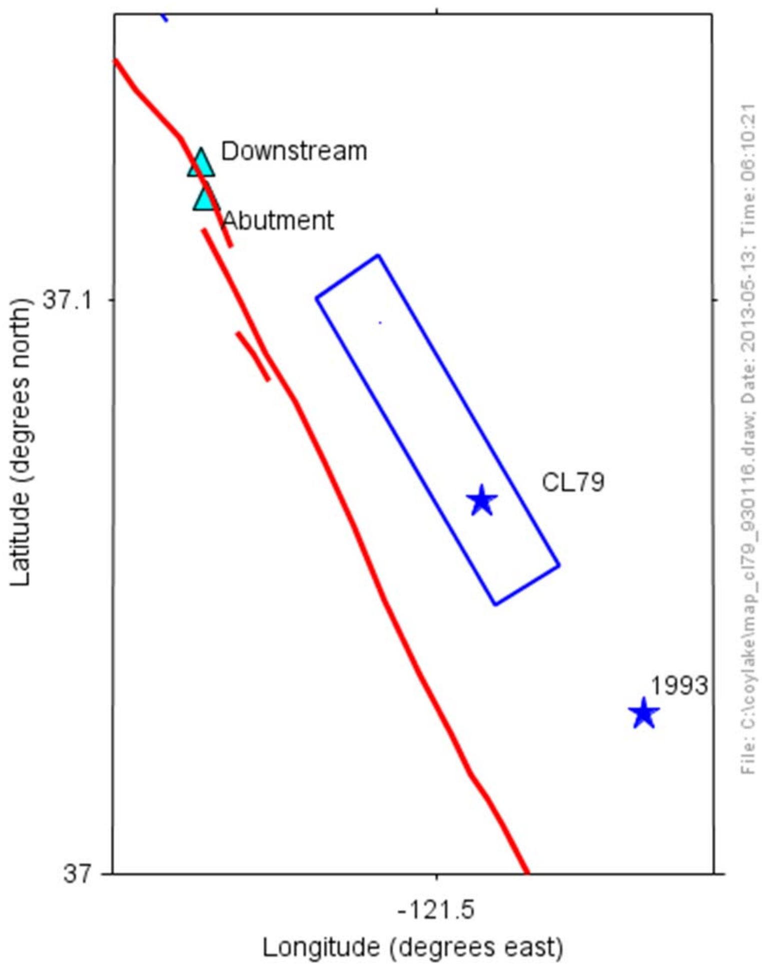

1993 (**M** 5.1): abutment, downstream

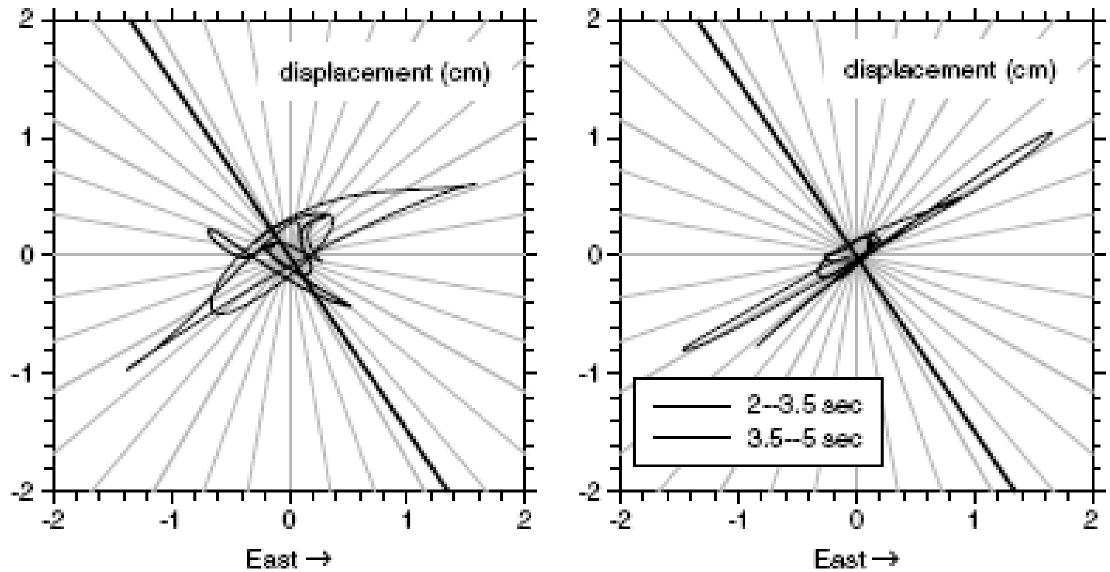

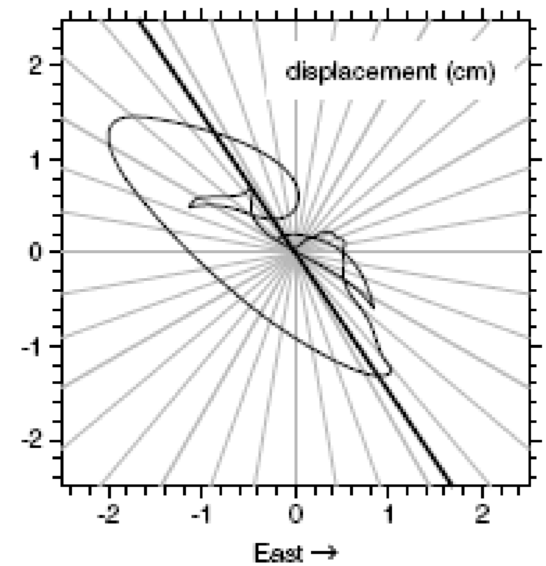

CL79 (**M** 5.7): abutment

Displacement frequencies ~0.5 to 2 Hz

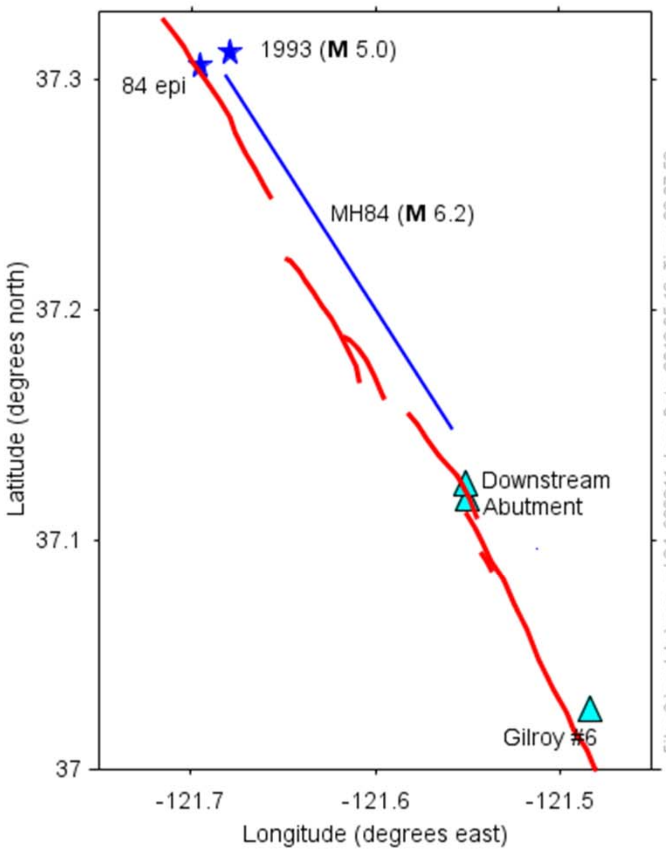

1993 abutment

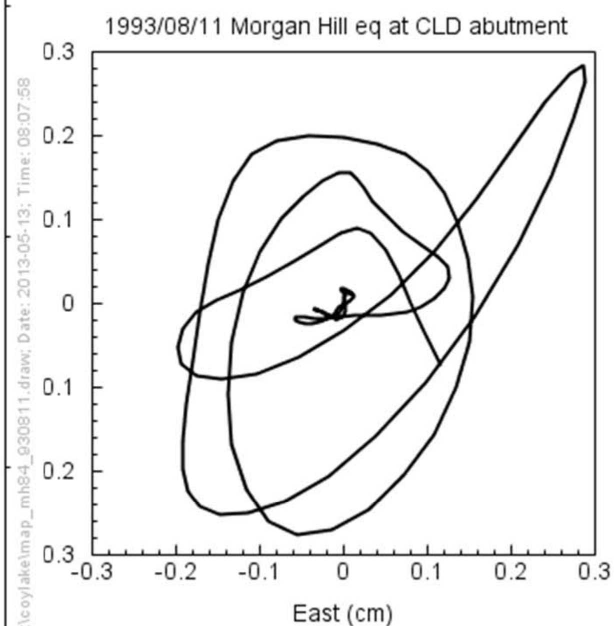

1993 downstream

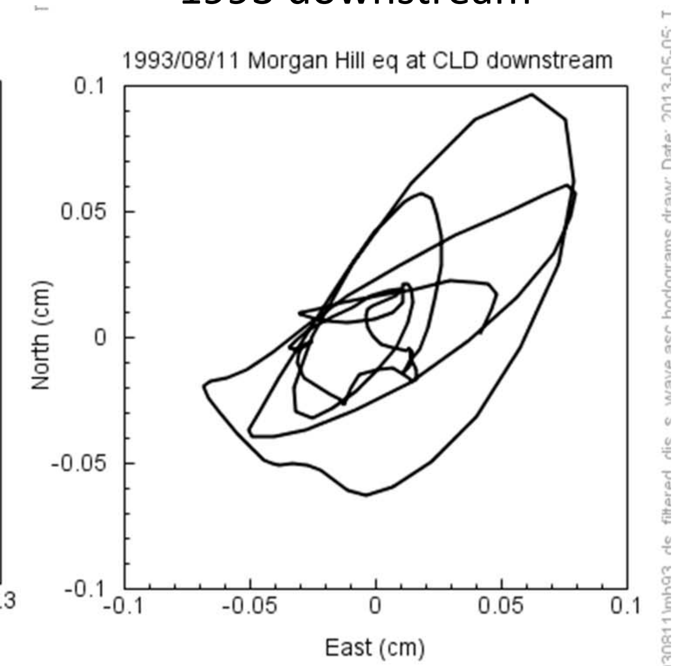

MH84

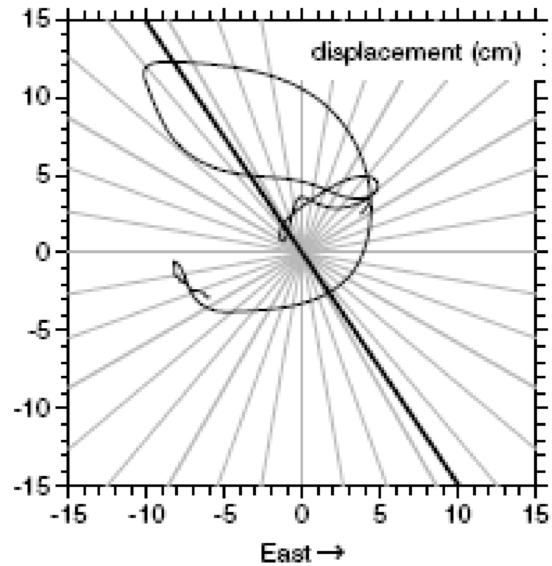

S-wave portion for 1993 is more fault normal than fault parallel, in contrast to MH84 at the abutment station

1984 Morgan Hill

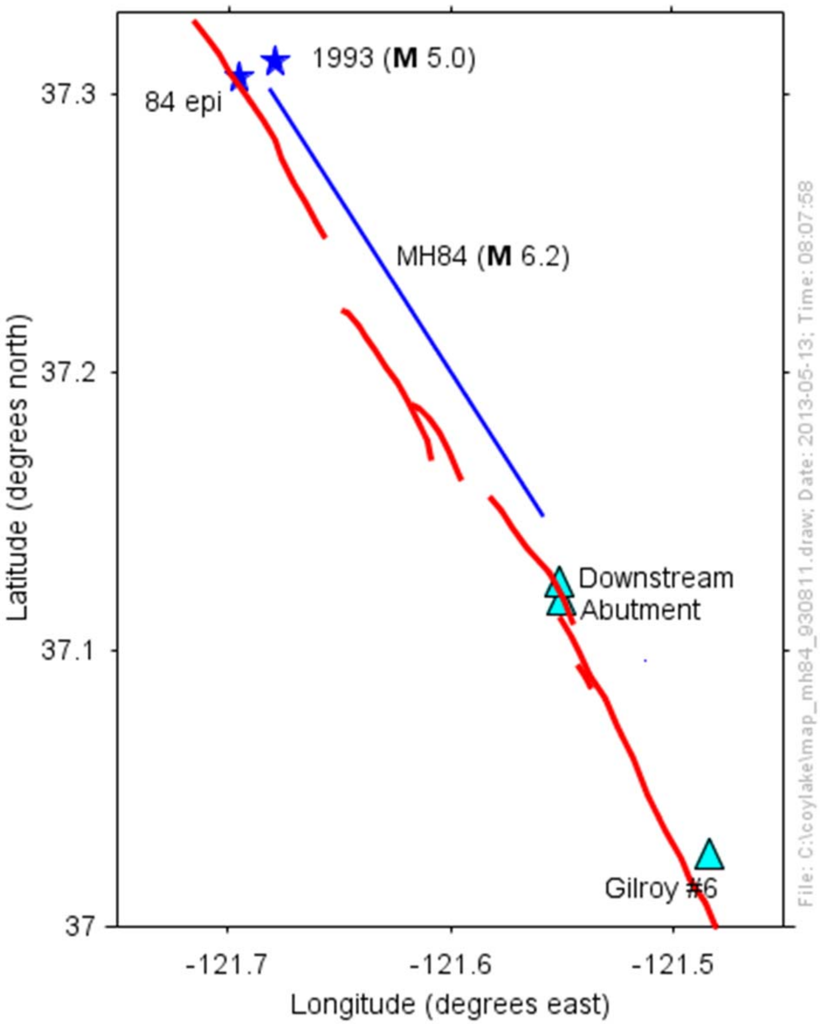

Abutment

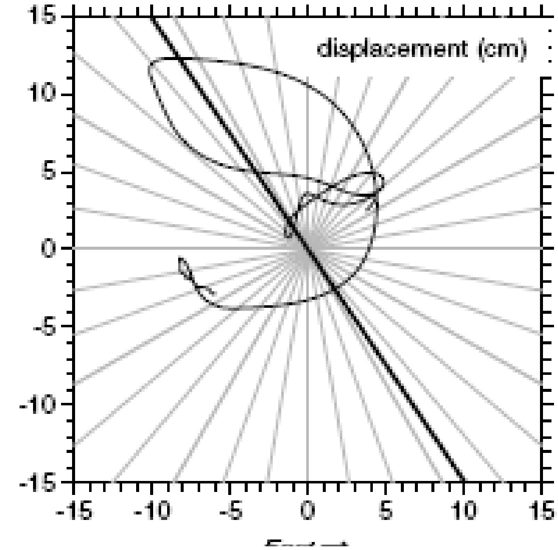

Gilroy #6

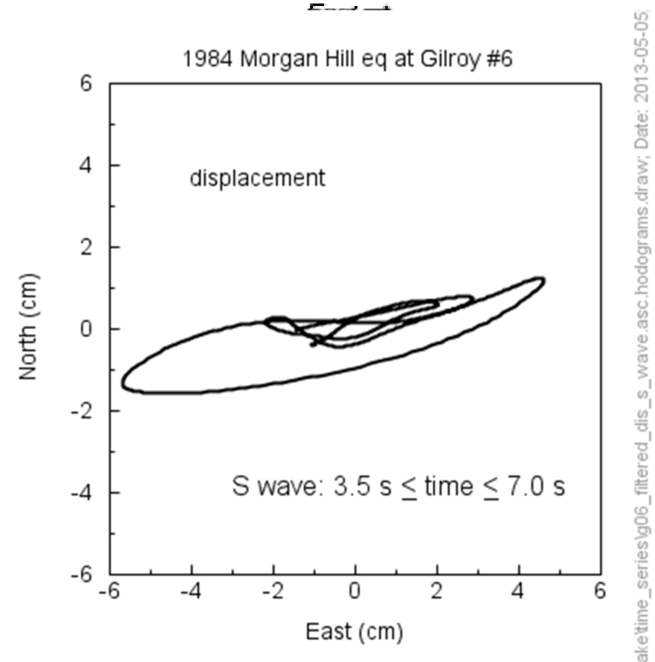

Sources of Variability of Amplitude and Polarization

- Nonuniform fault slip
- Site geology
- Fault zone effects

Turning now to GMPEs:

Number of records used for BSSA13 base-case GMPEs

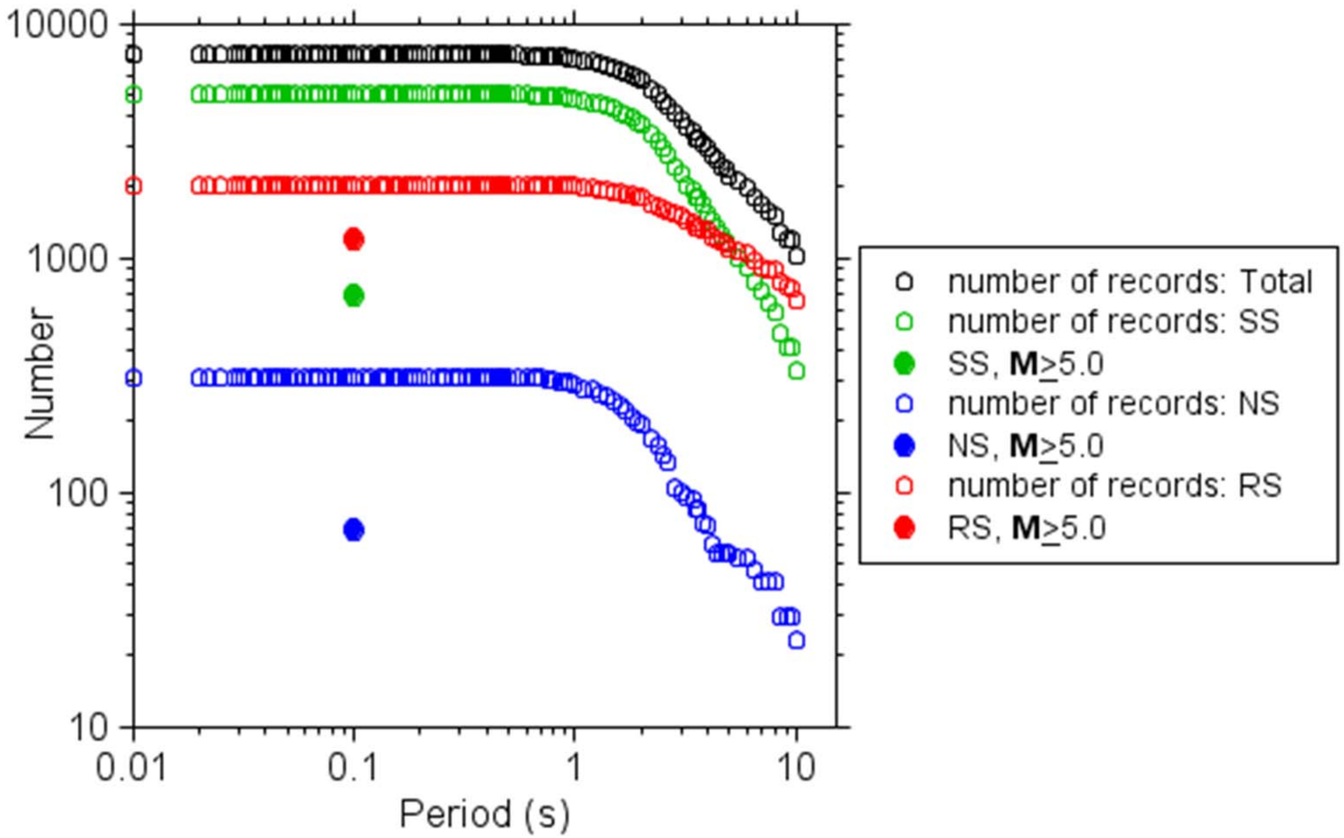

- SS only, adjusted to V_{S30}= 760 m/s
- Large scatter (**M**-dependent)
- For single **M**, near-source saturation
- Distance decay a function of period and **M** (not so obvious for **M**)
- For single R_{JB}, saturation for large **M**, close distances, short periods
- **M** scaling greater for long periods

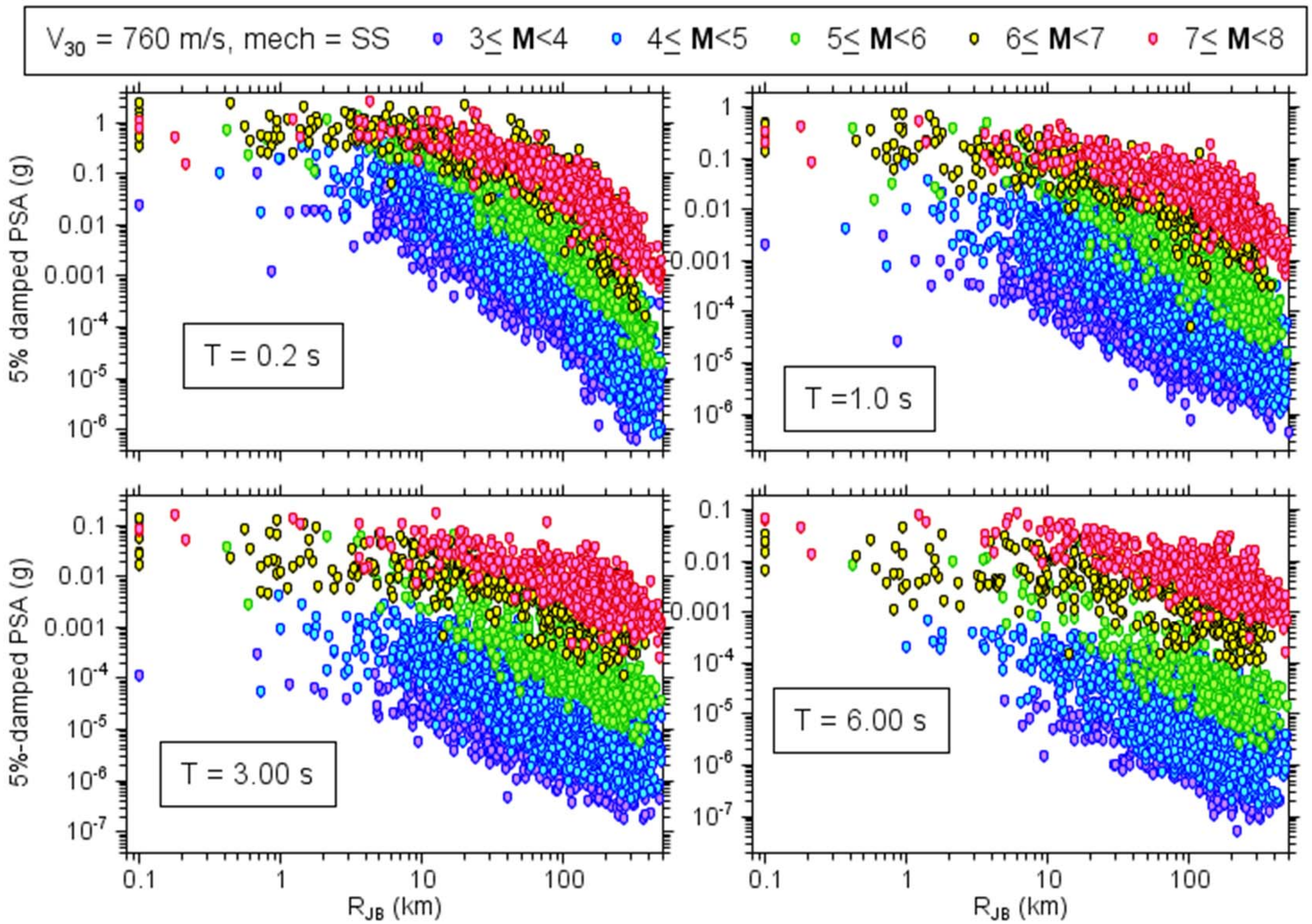

C:\nga_w2\report4peer_figures\ psa_vs_rjb.14mar13.m_3-4_4-5_5-6_6-7_7-8_vs_760_mech_1(ss)_t_0.2_1.0_3.0_6.0.draw

- For single **M**, near-source saturation
- Distance decay a function of period and **M** (not so obvious for **M**)
- For single R_{JB}, saturation for large **M**, close distances, short periods
- **M** scaling greater for long periods

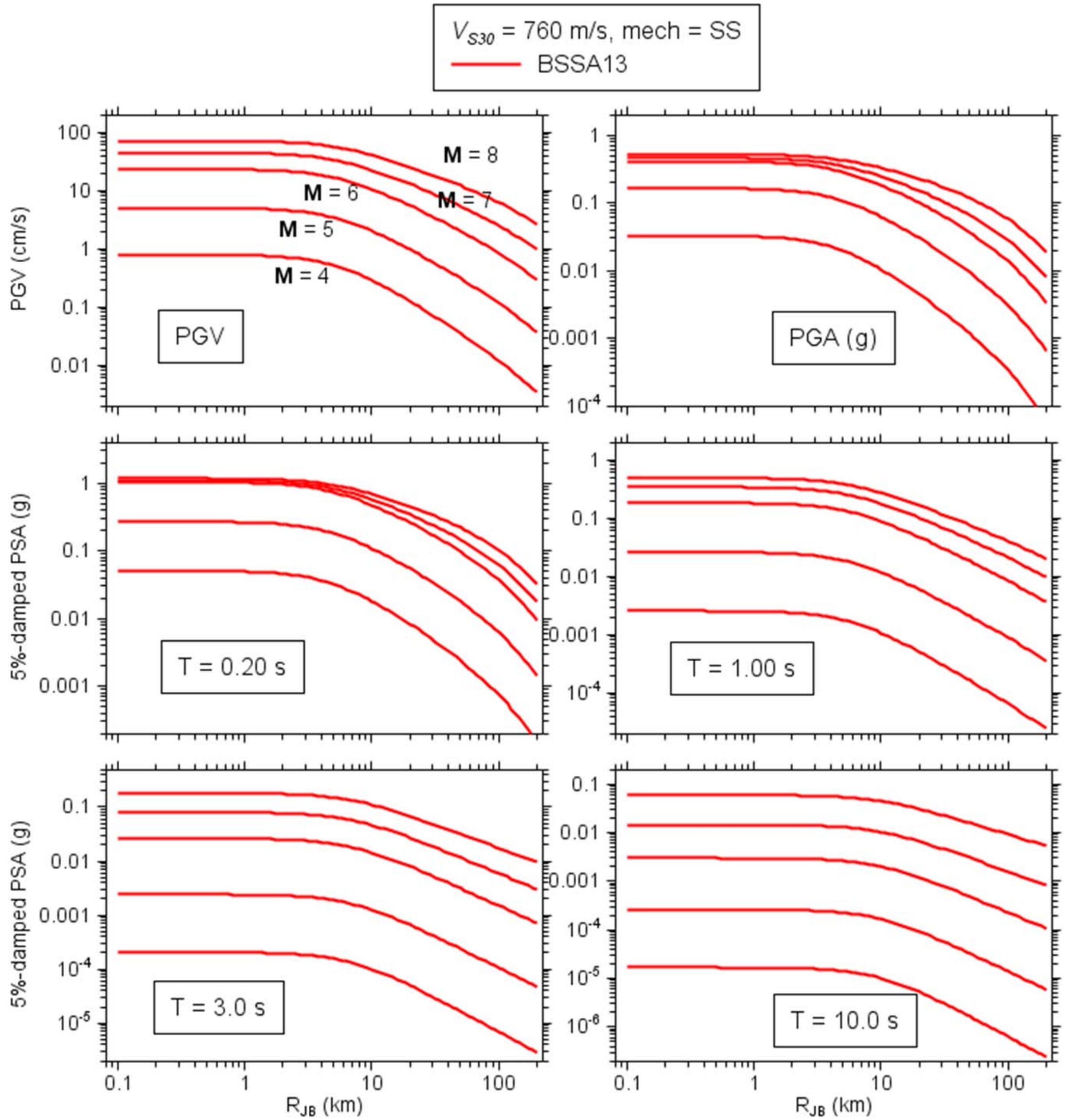

- Site amplification generally larger for long periods than short periods
- Nonlinear effects for large **M** (implying large “rock” motions) lead to reduction of motions at short periods

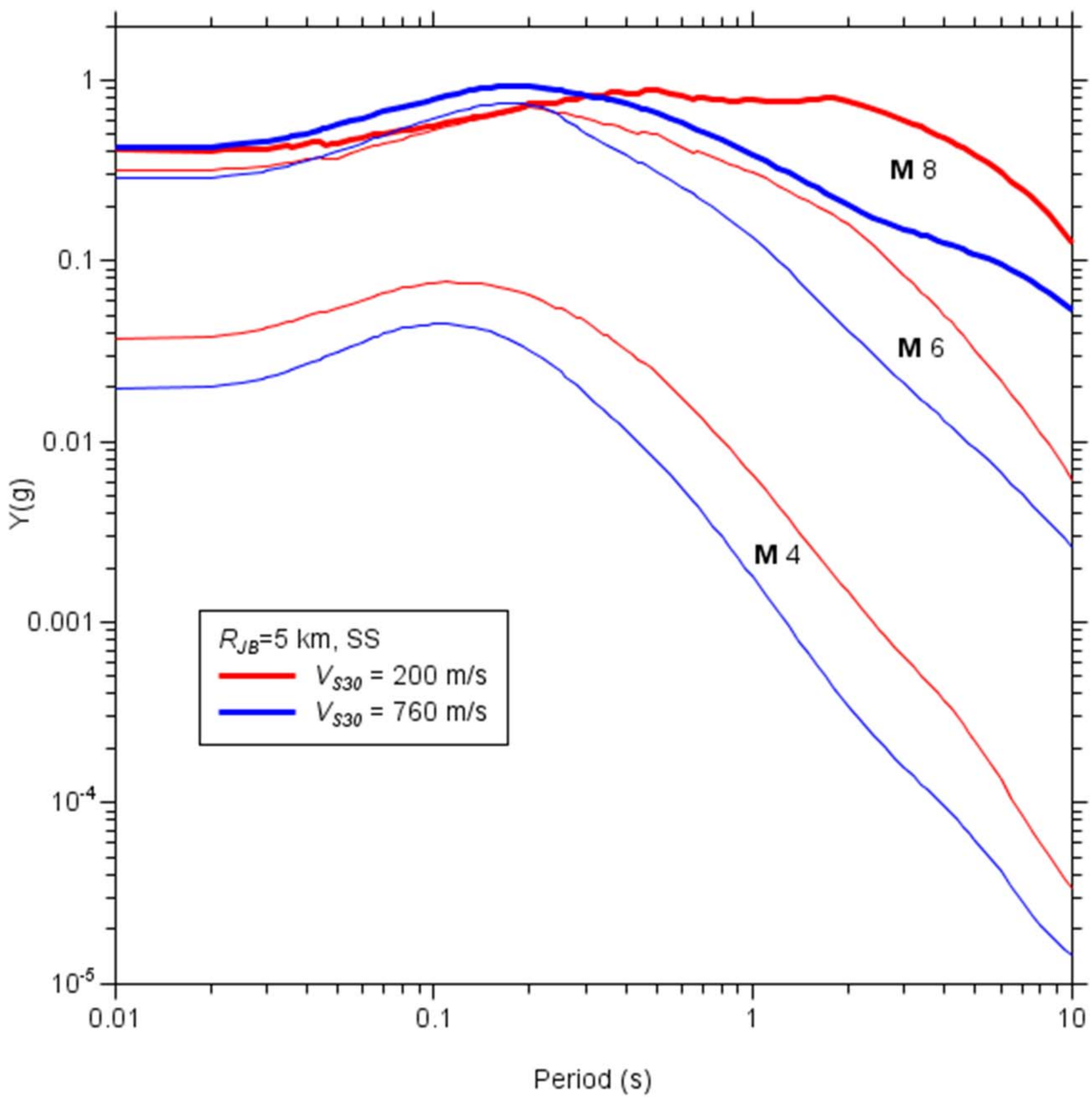

Scaling of Motions with Magnitude at Near and Intermediate Distances

- Data
- Data plus GMPEs
- Data plus simulations

SIMULATIONS

- Stochastic method fundamentals
- Finite-fault modification
- Source/path/site params for the simulations

Stochastic modelling of ground-motion: Point Source

- Deterministic modelling of high-frequency waves not possible (lack of Earth detail and computational limitations)
- Treat high-frequency motions as filtered white noise (Hanks & McGuire , 1981).
- combine deterministic target amplitude obtained from simple seismological model and quasi-random phase to obtain high-frequency motion. Try to capture the essence of the physics using simple functional forms for the seismological model**.** **Use empirical data when possible to determine the parameters**.

Basis of stochastic method

Radiated energy described by the spectra in the top graph is assumed to be distributed randomly over a duration given by the addition of the source duration and a distant-dependent duration that captures the effect of wave propagation and scattering of energy

These are the results of actual simulations; the only thing that changed in the input to the computer program was the moment magnitude (5 and 7)

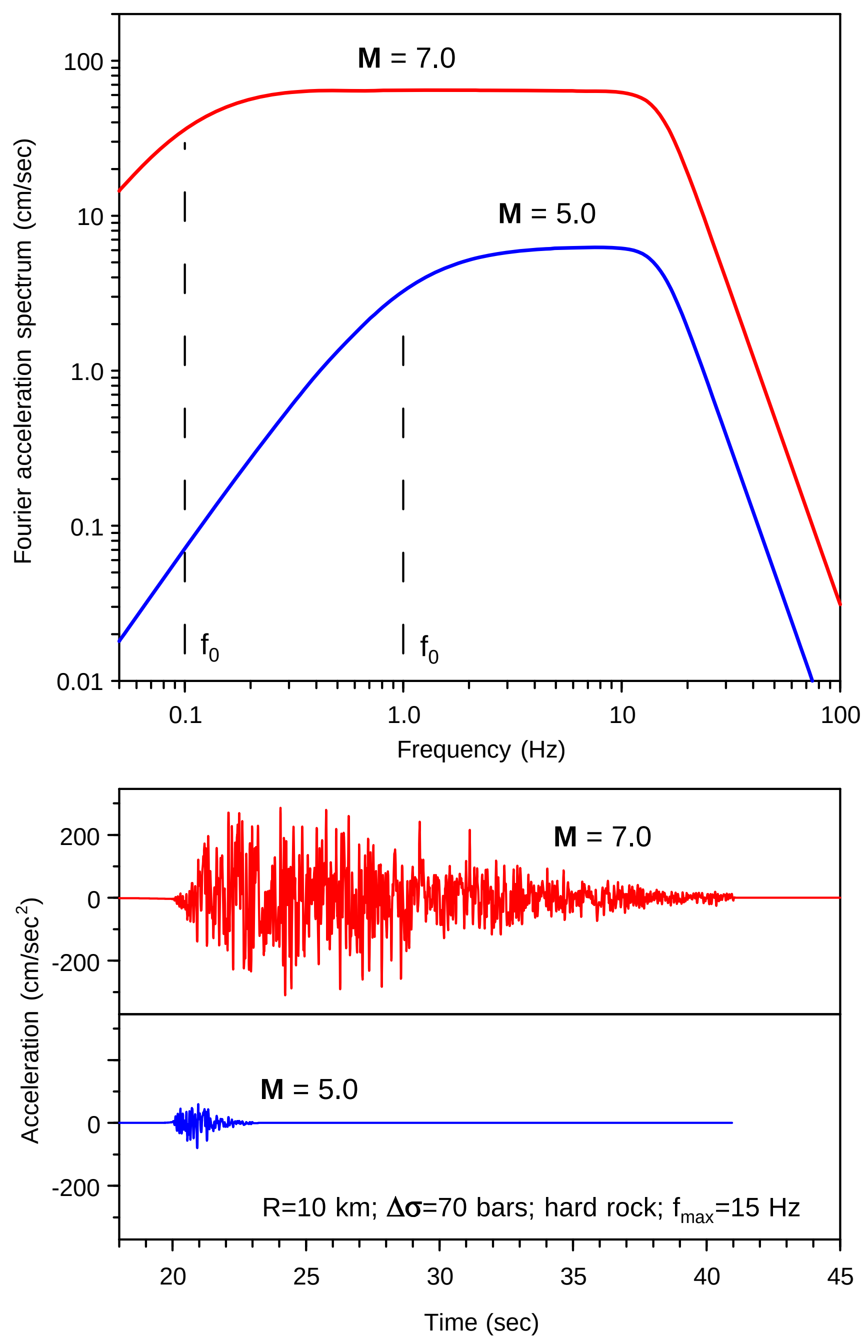

Target amplitude spectrum

Deterministic function of source, path and site characteristics represented by separate multiplicative filters

$$Y(M_0, R, f) = E(M_0, f) \times P(R, f) \times G(f) \times I(f)$$

Earthquake source

Propagation path

Site response

Instrument or ground motion

THE KEY TO THE SUCCESS OF THE MODEL LIES IN BEING ABLE TO DEFINE FOURIER ACCELERATION SPECTRUM AS F(M, DIST)

Finite-Fault Adjustments

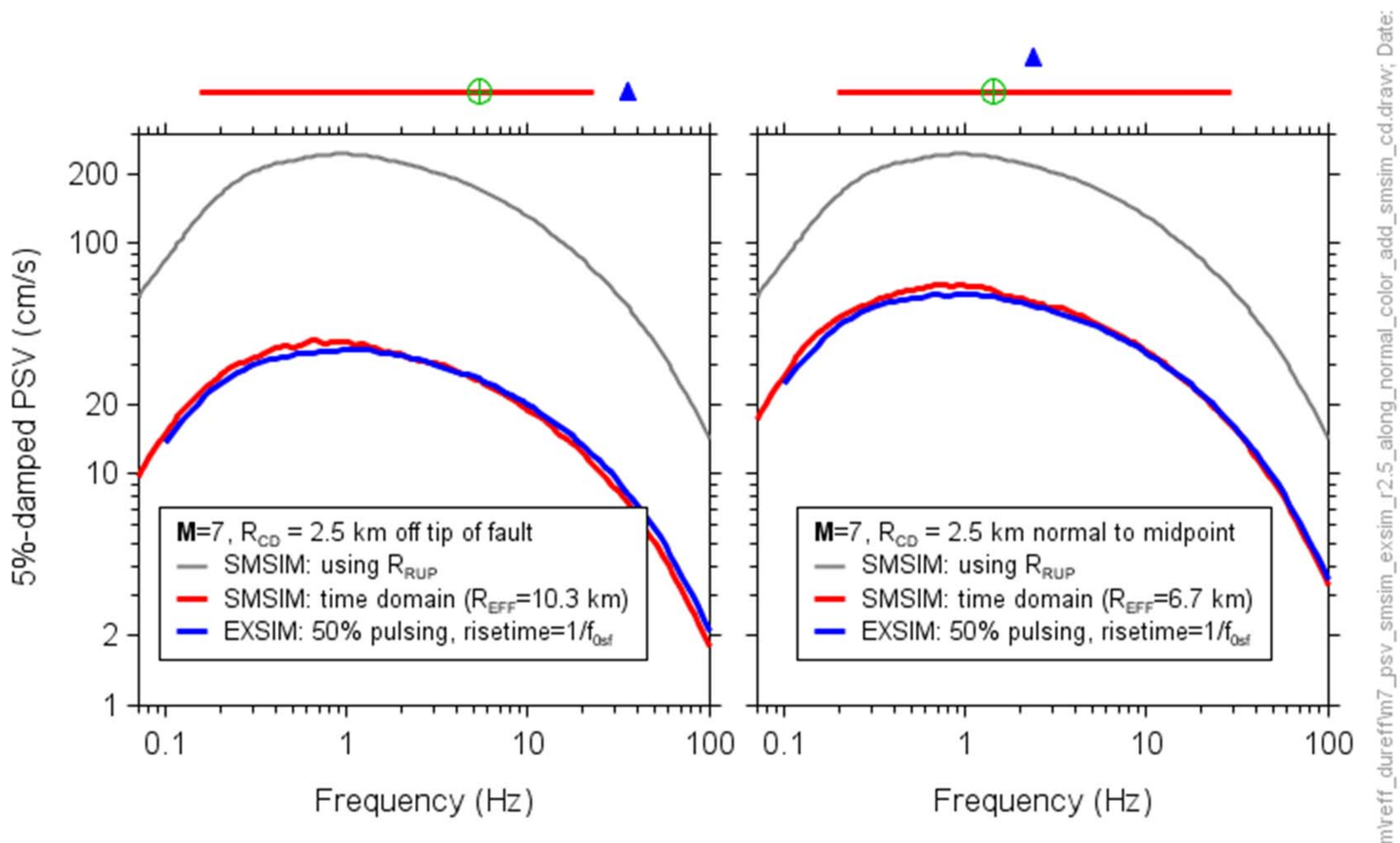

Parameters used in simulations are from Atkinson and Silva (2000)

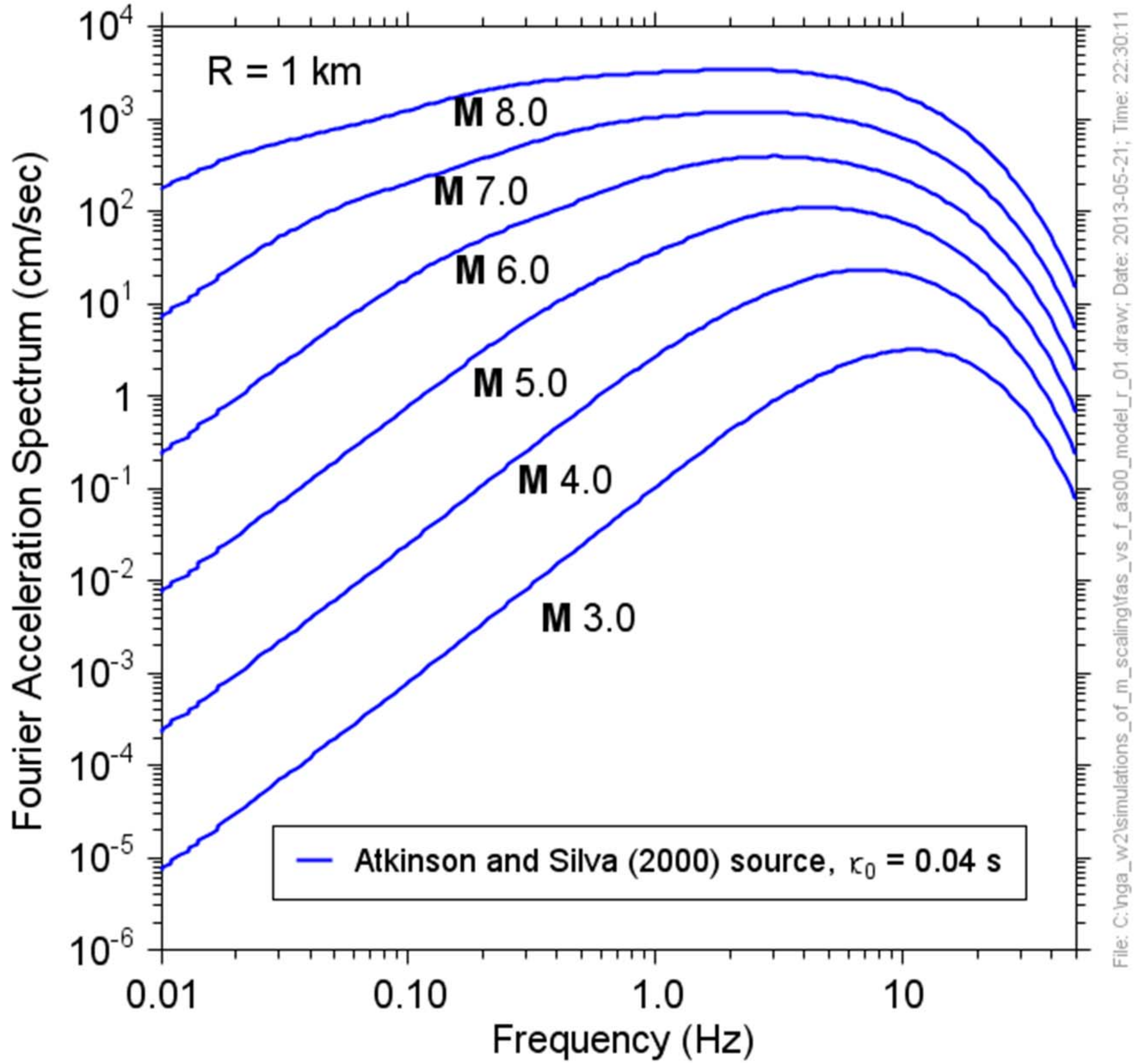

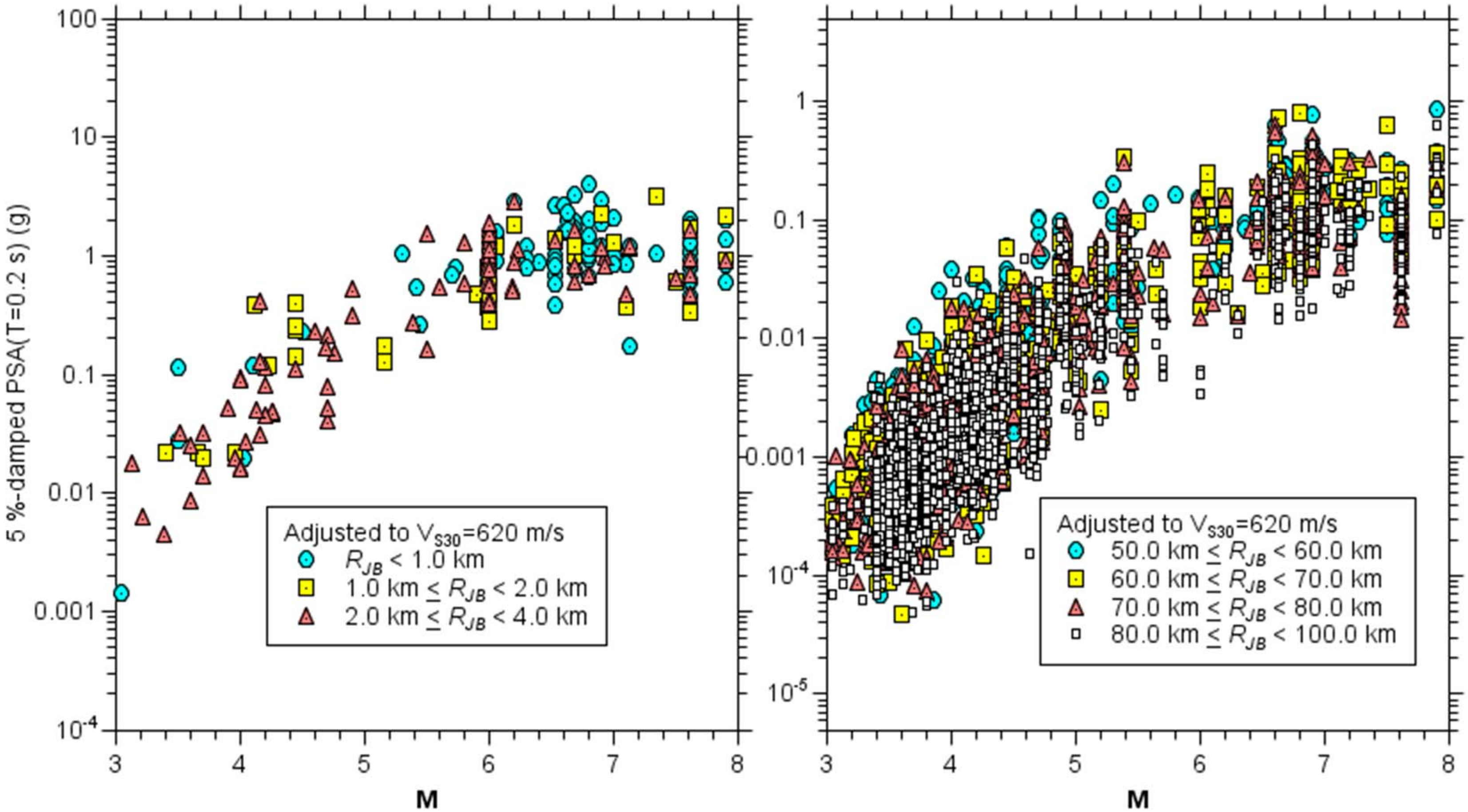

5 %-damped PSA(T=0.2 s) (g)
100
10
1
0.1
0.01
0.001
10^{-4}
3
4
5
6
7
8
M
Adjusted to V_{S30}=620 m/s
R_{JB} < 1.0 km
1.0 km ≤ R_{JB} < 2.0 km
2.0 km ≤ R_{JB} < 4.0 km
1
0.1
0.01
0.001
10^{-4}
10^{-5}
Adjusted to V_{S30}=620 m/s
50.0 km ≤ R_{JB} < 60.0 km
60.0 km ≤ R_{JB} < 70.0 km
70.0 km ≤ R_{JB} < 80.0 km
80.0 km ≤ R_{JB} < 100.0 km

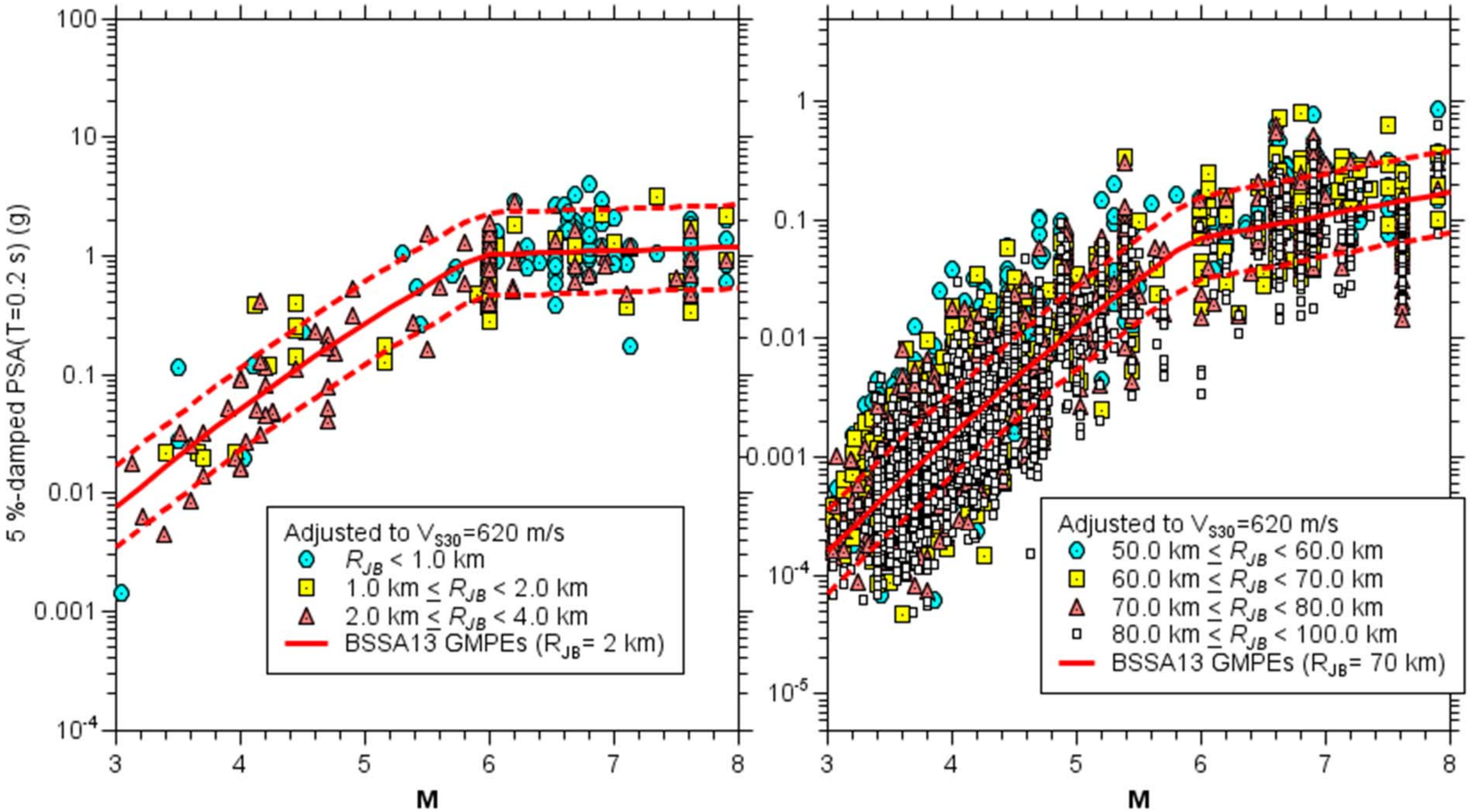

100
10
1
0.1
0.01
0.001
10^{-4}
5 %-damped PSA(T=0.2 s) (g)
3
4
5
6
7
8
M
Adjusted to V_{S30}=620 m/s
R_{JB} < 1.0 km
1.0 km ≤ R_{JB} < 2.0 km
2.0 km ≤ R_{JB} < 4.0 km
BSSA13 GMPEs (R_{JB}= 2 km)
1
0.1
0.01
0.001
10^{-4}
10^{-5}
Adjusted to V_{S30}=620 m/s
50.0 km ≤ R_{JB} < 60.0 km
60.0 km ≤ R_{JB} < 70.0 km
70.0 km ≤ R_{JB} < 80.0 km
80.0 km ≤ R_{JB} < 100.0 km
BSSA13 GMPEs (R_{JB}= 70 km)

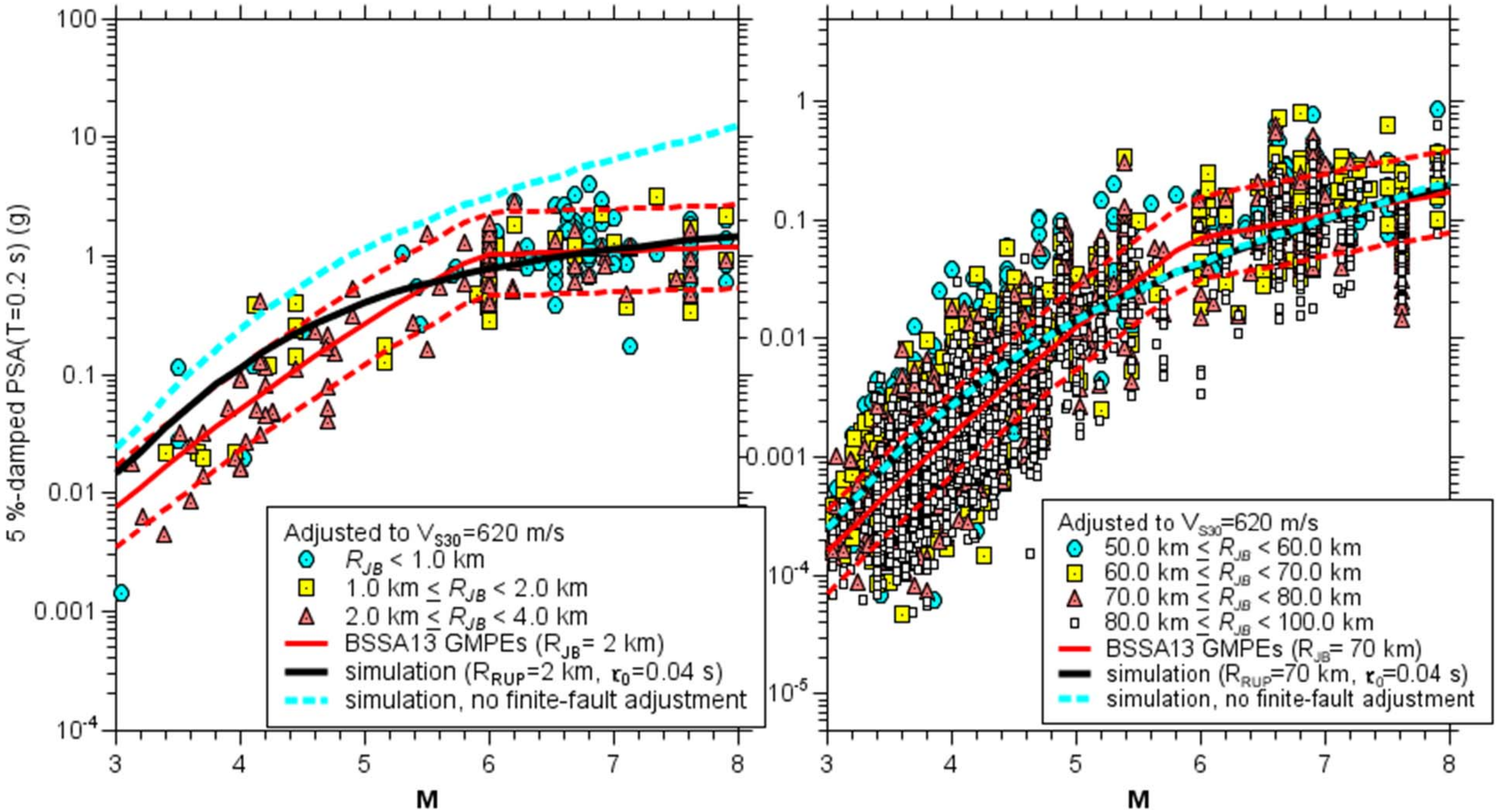

5 %-damped PSA(T=0.2 s) (g)
100
10
1
0.1
0.01
0.001
10^{-4}
3
4
5
6
7
8
M
Adjusted to V_{S30}=620 m/s
R_{JB} < 1.0 km
1.0 km ≤ R_{JB} < 2.0 km
2.0 km ≤ R_{JB} < 4.0 km
BSSA13 GMPEs (R_{JB}= 2 km)
simulation (R_{RUP}=2 km, κ_0=0.04 s)
simulation, no finite-fault adjustment
1
0.1
0.01
0.001
10^{-4}
10^{-5}
3
4
5
6
7
8
M
Adjusted to V_{S30}=620 m/s
50.0 km ≤ R_{JB} < 60.0 km
60.0 km ≤ R_{JB} < 70.0 km
70.0 km ≤ R_{JB} < 80.0 km
80.0 km ≤ R_{JB} < 100.0 km
BSSA13 GMPEs (R_{JB}= 70 km)
simulation (R_{RUP}=70 km, κ_0=0.04 s)
simulation, no finite-fault adjustment

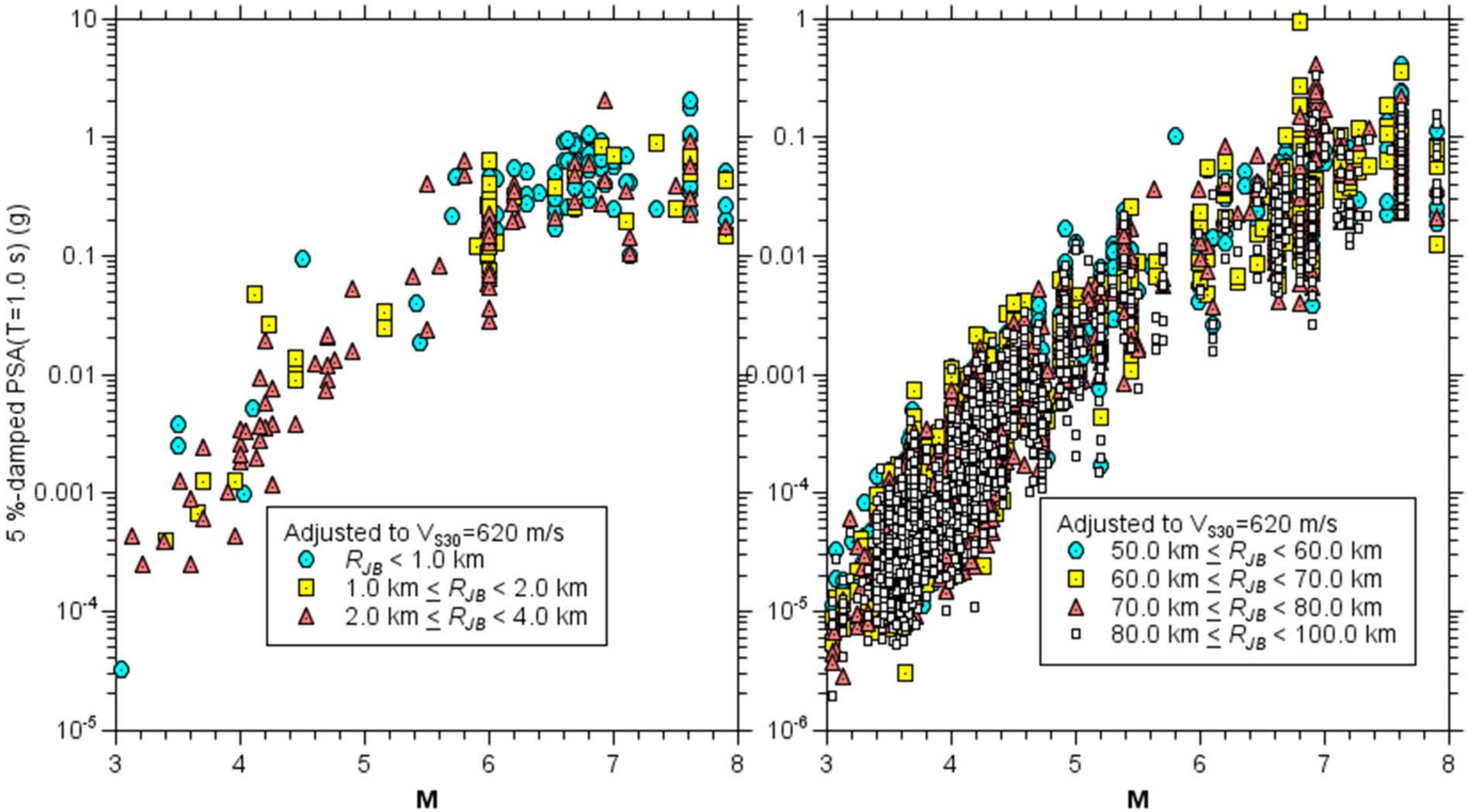
5 %-damped PSA(T=1.0 s) (g)
M
Adjusted to V_{S30}=620 m/s
R_{JB} < 1.0 km
1.0 km ≤ R_{JB} < 2.0 km
2.0 km ≤ R_{JB} < 4.0 km
Adjusted to V_{S30}=620 m/s
50.0 km ≤ R_{JB} < 60.0 km
60.0 km ≤ R_{JB} < 70.0 km
70.0 km ≤ R_{JB} < 80.0 km
80.0 km ≤ R_{JB} < 100.0 km

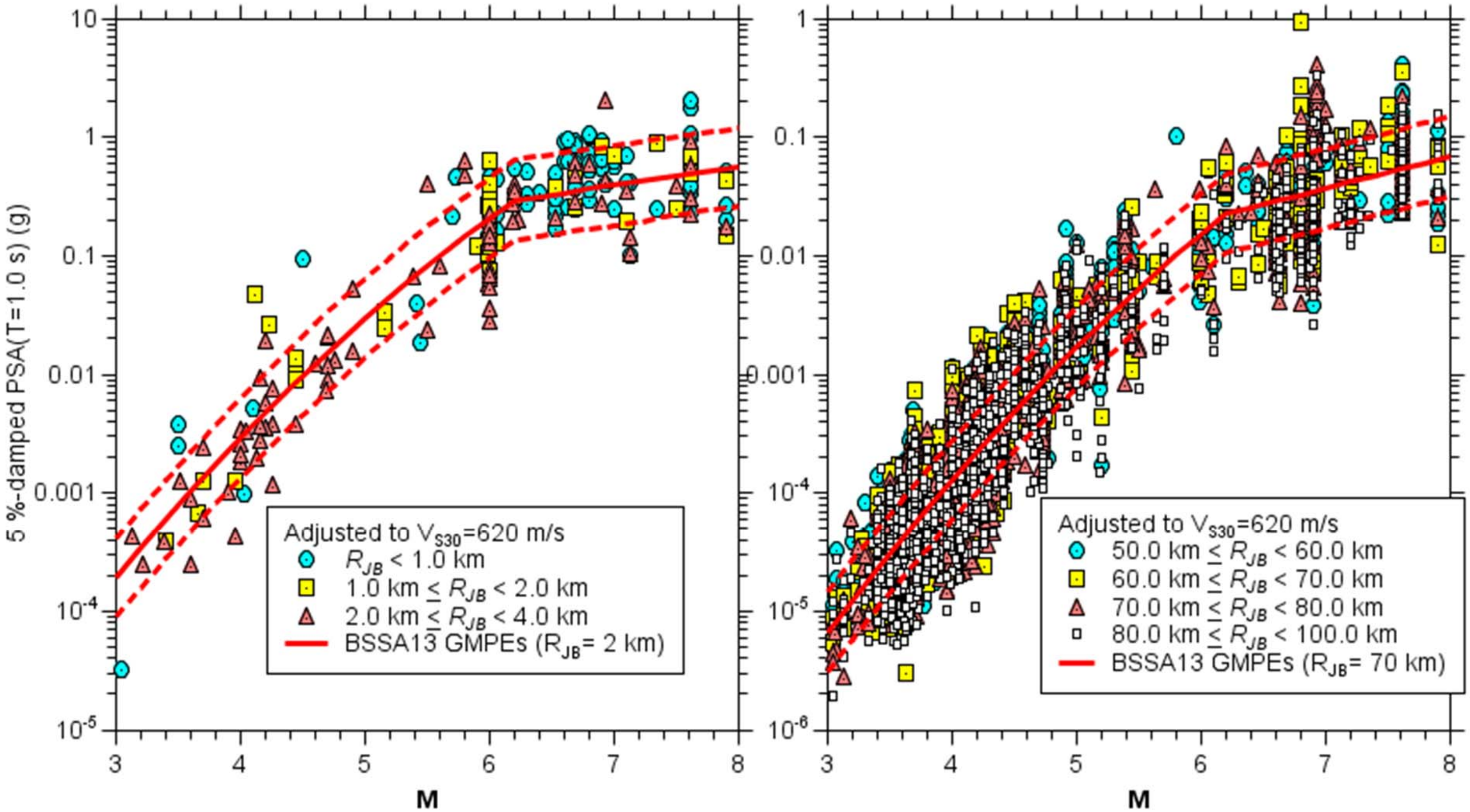
5 %-damped PSA(T=1.0 s) (g)
M
Adjusted to V_S30=620 m/s
R_JB < 1.0 km
1.0 km ≤ R_JB < 2.0 km
2.0 km ≤ R_JB < 4.0 km
BSSA13 GMPEs (R_JB= 2 km)
Adjusted to V_S30=620 m/s
50.0 km ≤ R_JB < 60.0 km
60.0 km ≤ R_JB < 70.0 km
70.0 km ≤ R_JB < 80.0 km
80.0 km ≤ R_JB < 100.0 km
BSSA13 GMPEs (R_JB= 70 km)

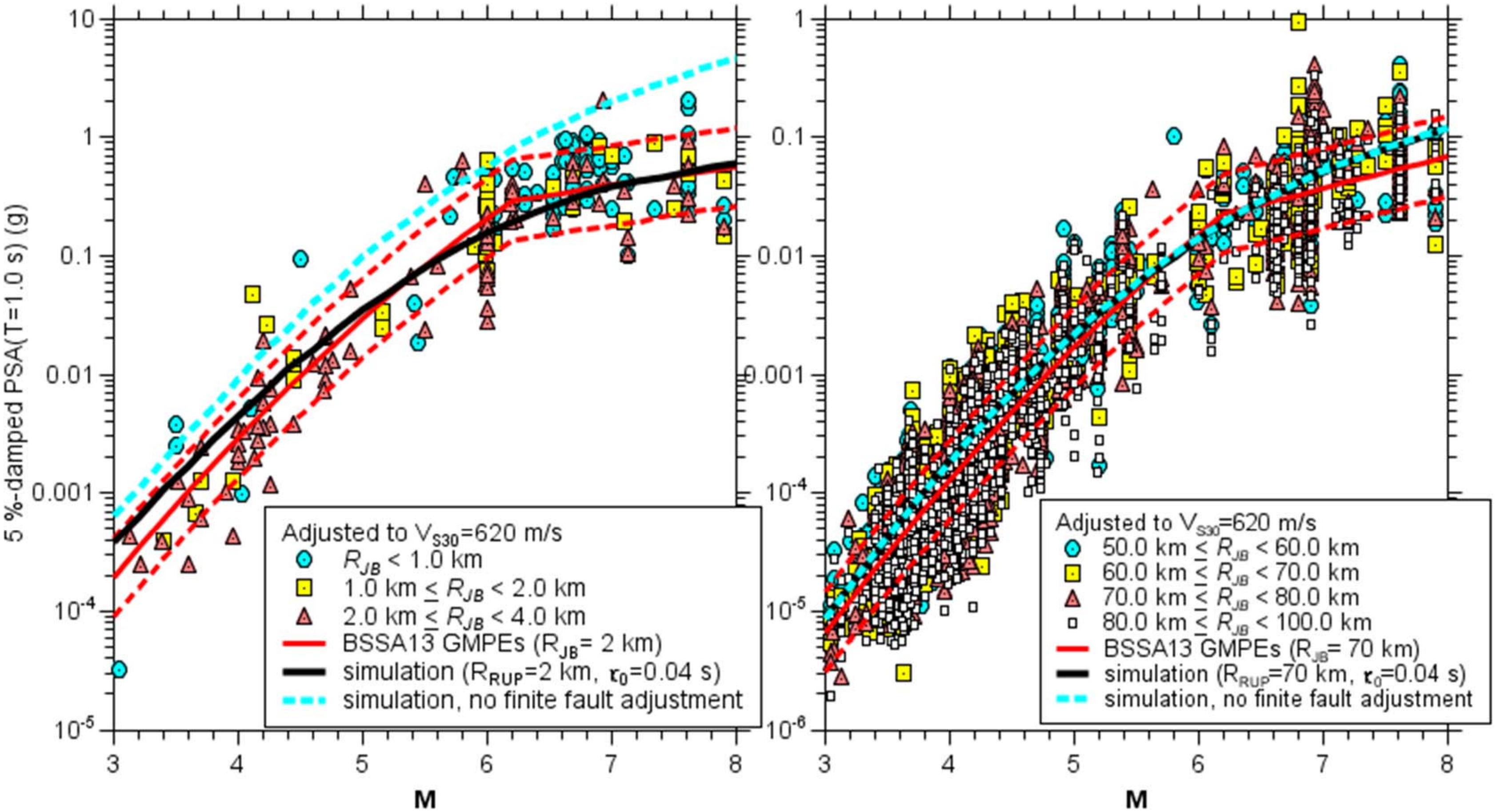

5 %-damped PSA(T=1.0 s) (g)
M
Adjusted to VS30=620 m/s
RJB < 1.0 km
1.0 km ≤ RJB < 2.0 km
2.0 km ≤ RJB < 4.0 km
BSSA13 GMPEs (RJB= 2 km)
simulation (RRUP=2 km, τ0=0.04 s)
simulation, no finite fault adjustment
Adjusted to VS30=620 m/s
50.0 km ≤ RJB < 60.0 km
60.0 km ≤ RJB < 70.0 km
70.0 km ≤ RJB < 80.0 km
80.0 km ≤ RJB < 100.0 km
BSSA13 GMPEs (RJB= 70 km)
simulation (RRUP=70 km, τ0=0.04 s)
simulation, no finite fault adjustment

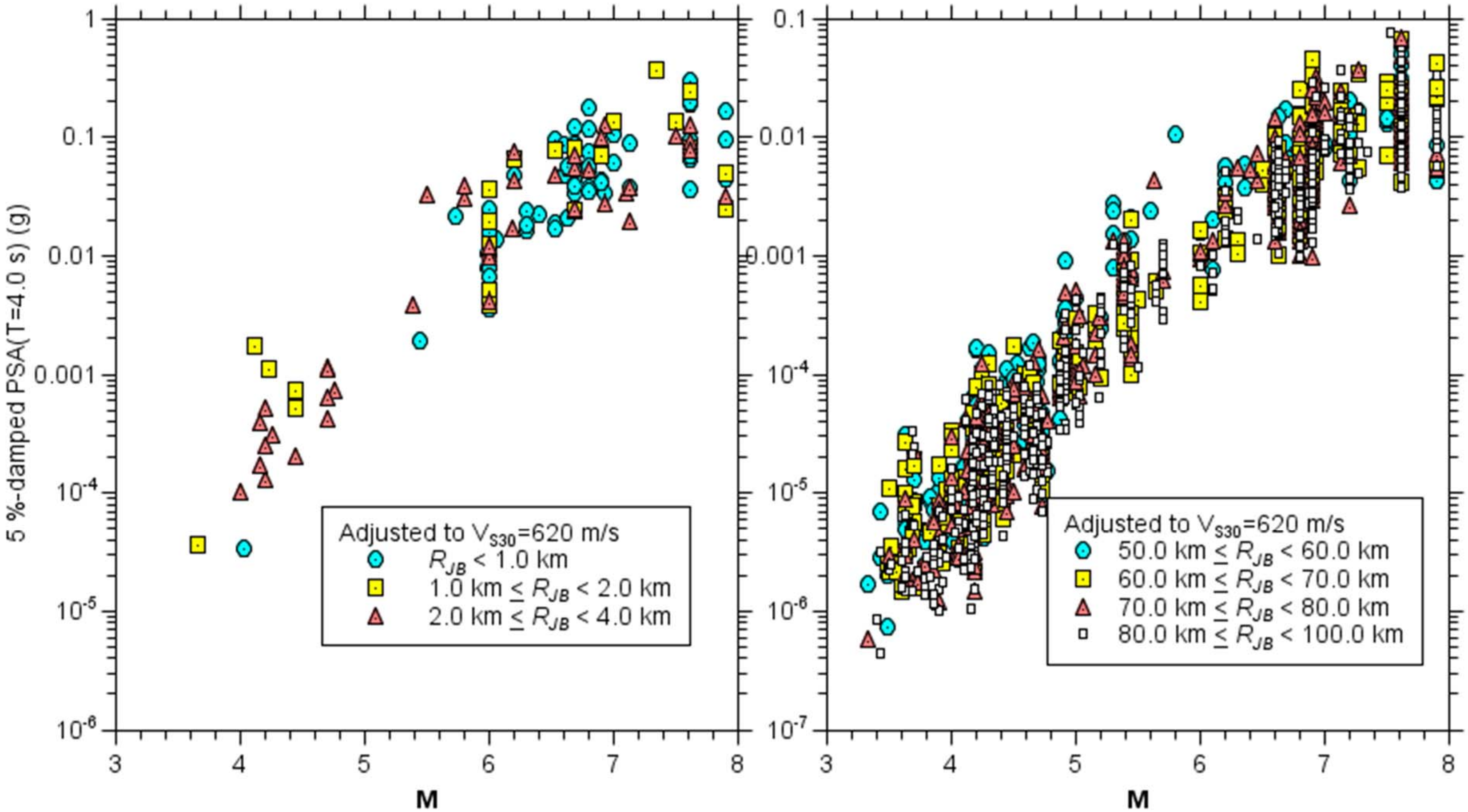

5 %-damped PSA(T=4.0 s) (g)
1
0.1
0.01
0.001
10^-4
10^-5
10^-6
3
4
5
6
7
8
M
Adjusted to V_S30=620 m/s
R_JB < 1.0 km
1.0 km ≤ R_JB < 2.0 km
2.0 km ≤ R_JB < 4.0 km
0.1
0.01
0.001
10^-4
10^-5
10^-6
10^-7
Adjusted to V_S30=620 m/s
50.0 km ≤ R_JB < 60.0 km
60.0 km ≤ R_JB < 70.0 km
70.0 km ≤ R_JB < 80.0 km
80.0 km ≤ R_JB < 100.0 km

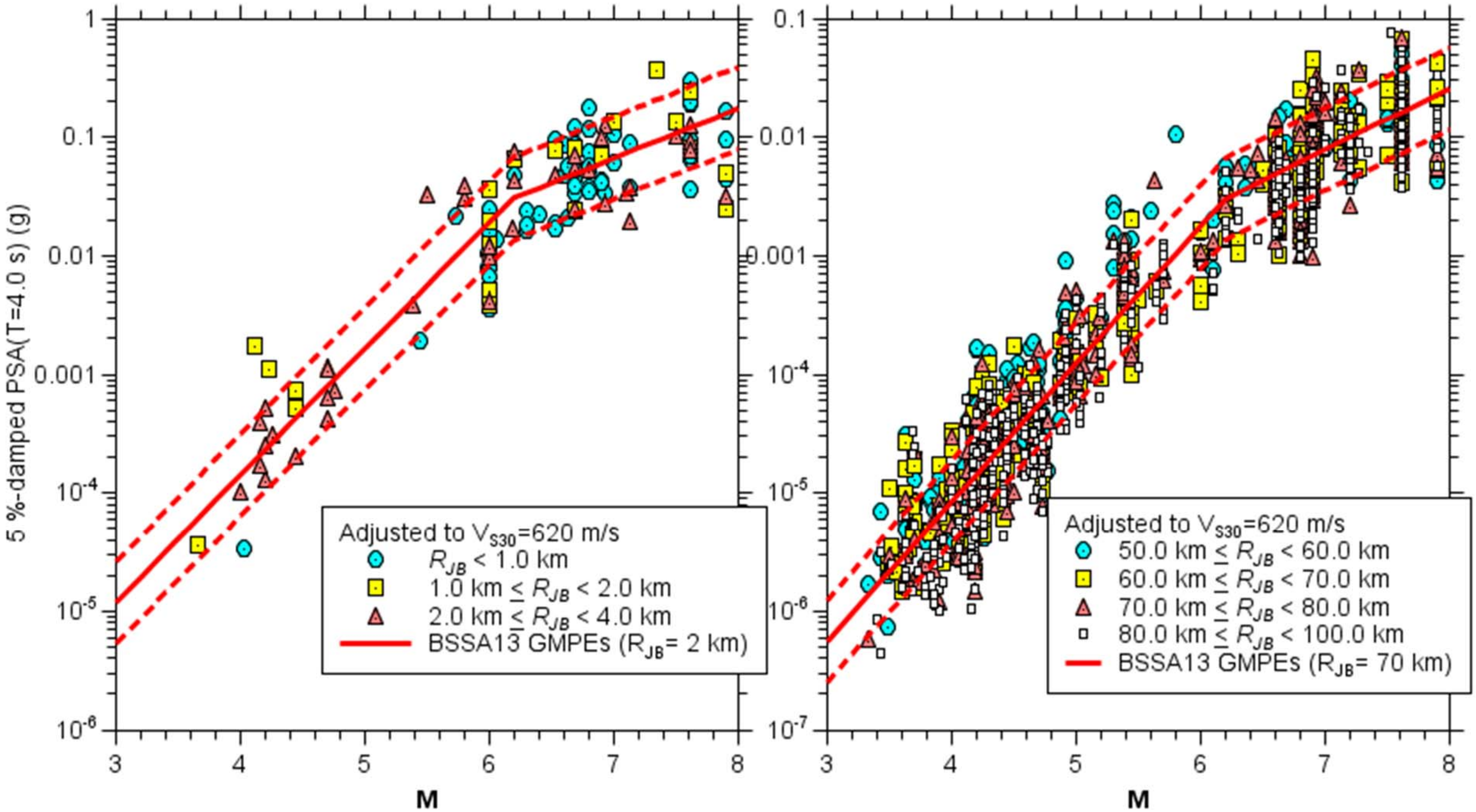

5 %-damped PSA(T=4.0 s) (g)
M
Adjusted to V_{S30}=620 m/s
R_{JB} < 1.0 km
1.0 km ≤ R_{JB} < 2.0 km
2.0 km ≤ R_{JB} < 4.0 km
BSSA13 GMPEs (R_{JB}= 2 km)
Adjusted to V_{S30}=620 m/s
50.0 km ≤ R_{JB} < 60.0 km
60.0 km ≤ R_{JB} < 70.0 km
70.0 km ≤ R_{JB} < 80.0 km
80.0 km ≤ R_{JB} < 100.0 km
BSSA13 GMPEs (R_{JB}= 70 km)

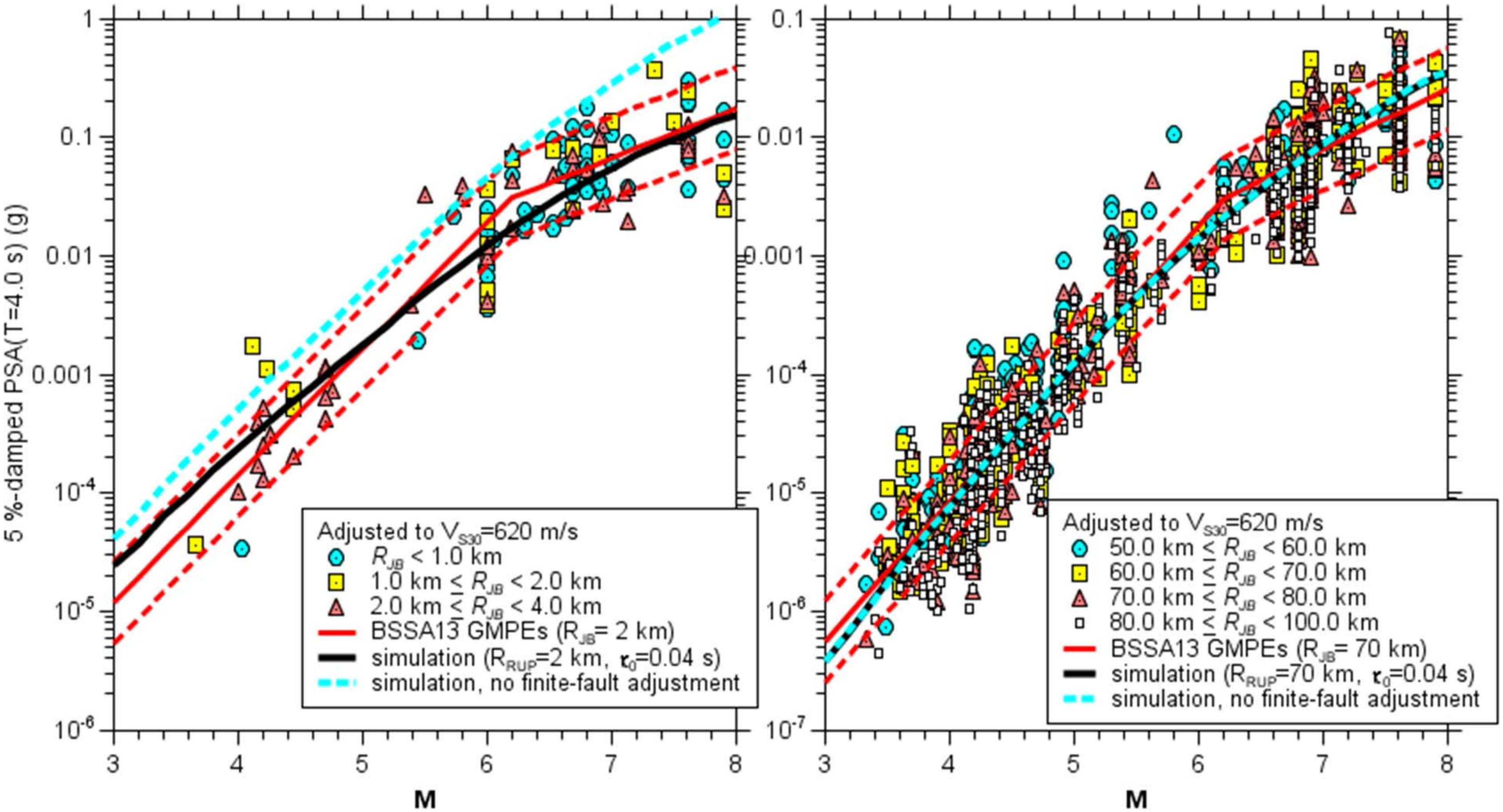

5 %-damped PSA(T=4.0 s) (g)
M
Adjusted to VS30=620 m/s
RJB < 1.0 km
1.0 km ≤ RJB < 2.0 km
2.0 km ≤ RJB < 4.0 km
BSSA13 GMPEs (RJB= 2 km)
simulation (RRUP=2 km, τ0=0.04 s)
simulation, no finite-fault adjustment
Adjusted to VS30=620 m/s
50.0 km ≤ RJB < 60.0 km
60.0 km ≤ RJB < 70.0 km
70.0 km ≤ RJB < 80.0 km
80.0 km ≤ RJB < 100.0 km
BSSA13 GMPEs (RJB= 70 km)
simulation (RRUP=70 km, τ0=0.04 s)
simulation, no finite-fault adjustment

Summary

- In spite of the large dataset, there are relatively few records from crustal fault zones in the large NGA dataset
- Fault zone records show significant variability in amplitude and polarization, but unraveling the causes of this variability is difficult
- The magnitude-to-magnitude increase of motions at a given distance becomes smaller as magnitude increases, with short-period motions at near-fault distances having almost complete saturation for large magnitudes
- The magnitude scaling is largely reproduced by simple models of the source and path effects

Thank you